



## Optimizing the amount of concentration and temperature of substances undergoing chemical reaction using response surface methodology

Shadi Bolouki Far<sup>a</sup>, Seyyed Amirreza Abdollahi<sup>b</sup>, As'ad Alizadeh<sup>c</sup>, Arsam Bostani<sup>d</sup>, Hussein Zekri<sup>e,g</sup>, Pooya Pasha<sup>f</sup>, Hossein Nabi<sup>f,\*</sup>

<sup>a</sup> New York Institute of technology, New York, United States of America

<sup>b</sup> Master student- Mechanical Engineering- Energy conversion-Faculty of mechanical engineering, Tabriz University, Tabriz, Iran

<sup>c</sup> Department of Civil engineering, College of Engineering, Cihan University-Erbil, Erbil, Iraq

<sup>d</sup> Department of mechanical engineering of bio systems, Urmia University, Iran

<sup>e</sup> Department of mechanical engineering, College of engineering, University of Zakho, Zakho, Kurdistan Region-Iraq

<sup>f</sup> Department of mechanical engineering Mazandaran University of science and technology, Babol, Iran

<sup>g</sup> College of Engineering, The American University of Kurdistan, Duhok, Kurdistan Region-Iraq

### ARTICLE INFO

#### Keywords:

Finite element method  
Reaction and diffusion  
Design - expert  
Arrhenius equations

### ABSTRACT

In this article, we investigate the temperature and concentration of particles around a vessel in three different locations using the reaction and diffusion relations, the reaction between three chemical particles, and the relationship between temperature changes and the rate of chemical reaction. The goal and necessity of this research is that we were able to visualize these chemical agents by using a finite mathematical fluid method, changing the physical properties of the materials, and learning about how chemical reactions affect concentration and temperature and how they relate to one another. The innovation of this essay is that it compares the parameters of concentration and temperature of substances involved in chemical reactions in different places of the inner vessel to the larger vessel, with and without the presence of a heat source. We also achieved the highest and best efficiency of concentration and heat transfer of chemical reactions (a), (b), and (c) using the finite method in Flexpde, Ansys fluent, and Design - Expert software (c). The obtained results show that the concentration changes significantly as the temperature of the reactants rises and more heat is released. According to the test conducted with the RSM method, the best efficiency and optimization of temperature and concentration parameters occurs in heat source = 2.555°, diffusivity = 0.025 and diameter of inner vessel = 3.144 cm.

### 1. Introduction

In this article, we utilize the reaction and diffusion relations and the relationship between temperature changes and the rate of chemical reaction to investigate the temperature and concentration of particles around a vessel in the three different places. Reaction-diffusion models are scientific models which compare to some amazing physical phenomena. The most common are spatial and temporal changes in the concentration of one or more chemical species: adjacent chemical reactions in which species transform into each other, and diffusion, which results in the diffusion of species across surfaces in space. Reaction-diffusion theory is connected to chemistry. Regardless of the framework, non-chemical forms of dynamism can be portrayed. Cases are found in many different scientific disciplines, including science,

geography, and material science. The neutron dissemination hypothesis is one example of a case study in biology. Numerically, reaction-diffusion frameworks take the perspective of semi-linear allegorical halfway differential conditions. Many researchers such as Abdollahzadeh, Sadeqi, and Fakhimi and their colleagues in the field of mechanics of fluids and solids and many researchers in chemical processes (on the density of eutectic solvents, analysis on the incompressible flow field around the solid cylinder and the thermodynamic model of the hydrogen storage tank with CFD) did [1–8]. Industrial chemistry, reactions, and diffusion relations have helped in the discovery and improvement of modern and advanced industrial filaments, paints, cement, drugs, cosmetics, electronic components, lubricants, and thousands of other items, as well as advanced forms for oil refining and petrochemicals that preserve vitality and reduces pollution. In this article, we will use Flexpde software to solve diffusion reactions in chemical relations, and for this

\* Corresponding author.

E-mail address: [azarheydari984@gmail.com](mailto:azarheydari984@gmail.com) (H. Nabi).

<https://doi.org/10.1016/j.ijft.2022.100270>

Nomenclature	
$K_b, K_a, K_c$	= diffusivities
$K_1$	= Reaction coef for $A + B$
$H_1$	= Activation energy/k for $A + B$
$K_2$	= Reaction coef for C
$H_2$	= Activation energy/k for C
$a_0, b_0, c_0$	= initial distribution
$tabs$	= Temp+273
$t\ fact\ 1$	= $K_1.exp(-H_1/tabs)$
$t\ fact\ 2$	= $K_2.exp(-H_2/tabs)$
$A, B, C$	= Component of chemical reactions
$T$	= Temperature

Arrhenius characterized a corrosive as a compound that increments the concentration of element particle ( $H +$ ) in equation arrangement. The Arrhenius condition is a few of the time communicated as  $k = Ae-E/RT$  wherever  $k$  is that the rate of chemical response,  $A$  may be a gradual looking on the chemicals included,  $E$  is the feat energy,  $R$  is the encompassing gas steady, and  $T$  is the temperature [17–21]. Shirvan and his colleagues [22–25] conducted research on topics such as heat exchangers and chemical reactions and equations of the energy domain by CFD fluid methods and numerical calculations. Khan and his colleagues investigated the modeling of fluid flow in body vessels analytically and numerically, as well as the flow of different nanofluids in and around the channels and the effects of electric currents on Jeffrey’s fluid [26–37]. The Leveraging a program called Flexpde and CFD, we were able to examine the concentration of reactants and products as well as changes in heat transfer to the center of the fluid by using relationships between the chemically coupled fluid equations and changes in a number of

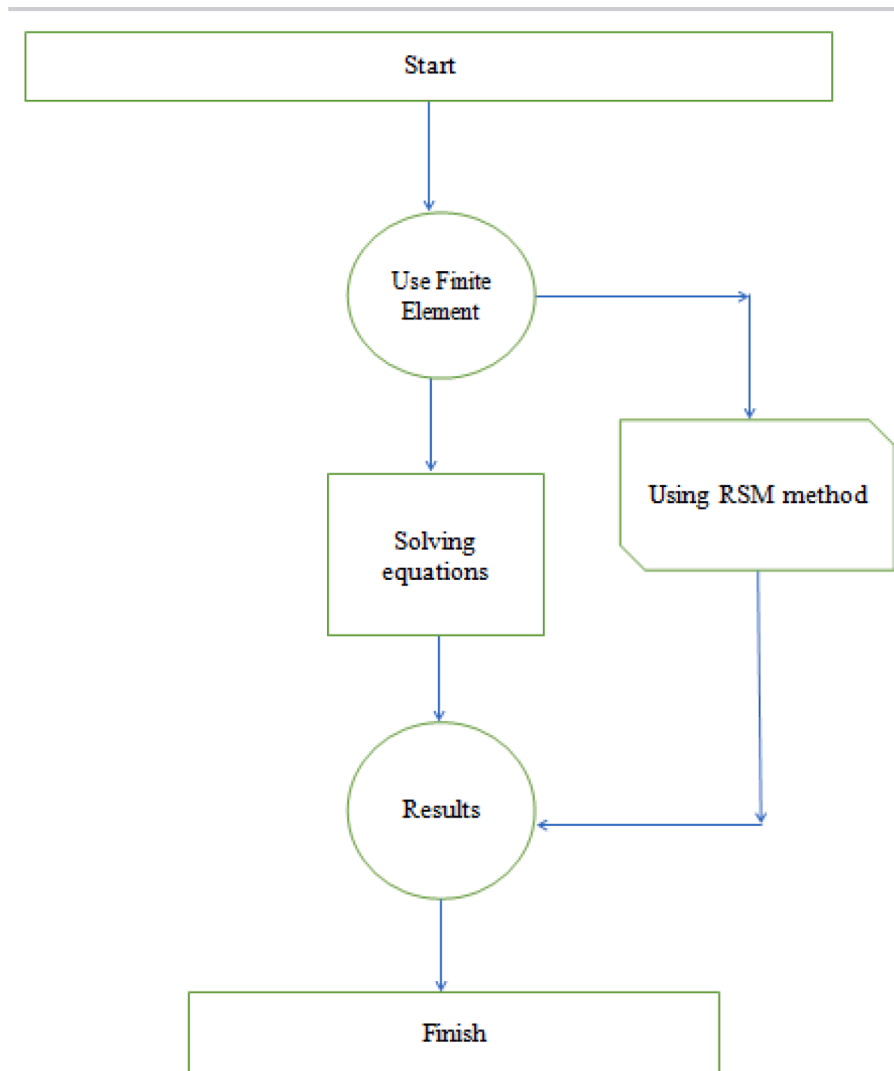


Fig 1. Grid study of the quandary.

purpose, we will explain the FEM method. The FEM [9–16] may be a common numerical strategy for tackling halfway differential conditions in two or three space factors. To unravel an issue, the FEM subdivides an expansive framework into littler; easier parts that are called limited components. The Swedish chemist Svante Arrhenius developed the primary chemical definitions of acids and bases in the late 1800s.

chemical parameters. We looked at the vessel’s shape, the temperatures in various parts of the vessel, and we displayed the heat flux at the boundaries. Additionally, the associations between temperature and concentration as well as the connection between reaction rate and these variables were examined. The goal and necessity of this research is that by using a finite mathematical fluid method, changing the physical

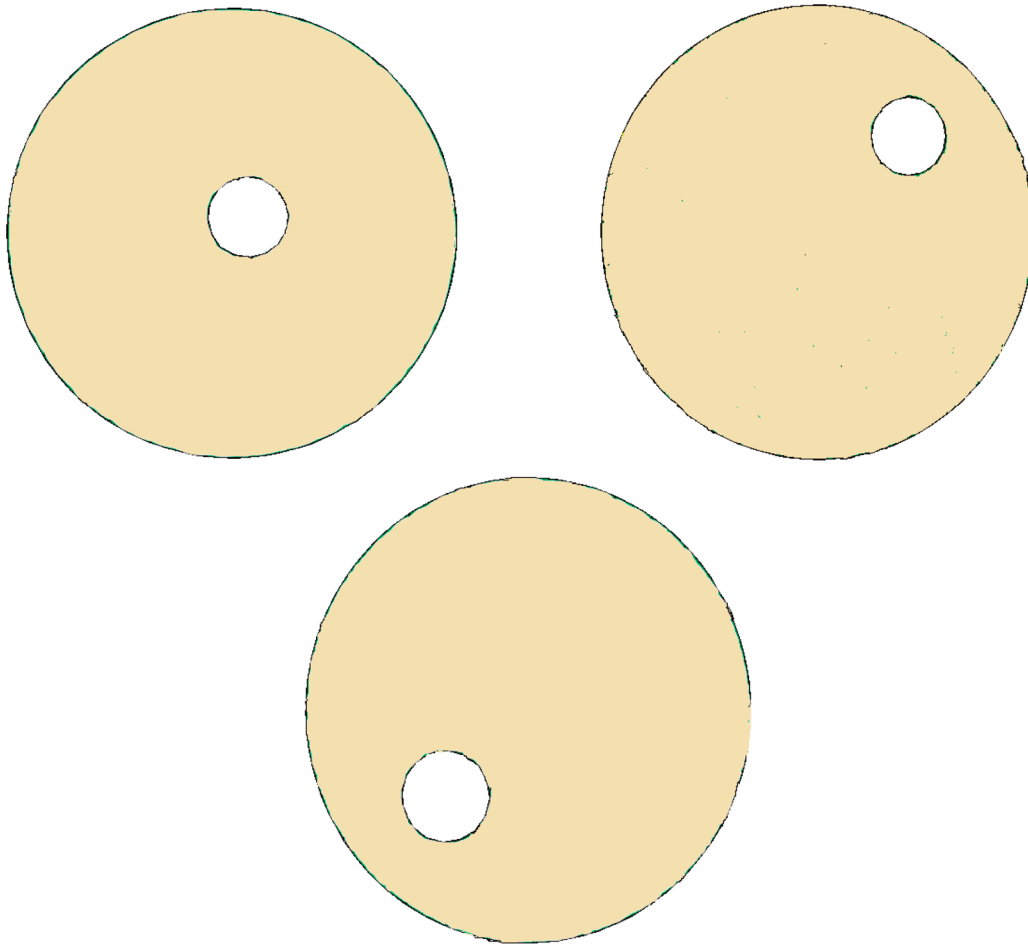


Fig 2. Geometry of the quandy.

properties of the materials, and learning about how chemical reactions affect concentration and temperature and how they relate to one another, we were able to visualize these chemical agents. The best efficiency can be achieved by reaction, reaction, and changes in heat transport. Also by using of Design expert software and RSM strategy, we optimize the temperature and concentration of chemical reaction by changing the diameter of the inner vessel and amount of heat sources. In this paper, using the reaction and diffusion relations and the reaction between 3 chemical particles and the relationship between temperature changes and the rate of chemical reaction, we investigate the temperature and concentration of particles around a vessel in the three different places. The novelty of this article is to examine the parameters of concentration and temperature of substances involved in chemical reactions in different places of the inner vessel compared to the larger vessel Fig. 1.

## 2. Problem definition

In this paper, using the reaction and diffusion relations and the reaction between 3 chemical particles and the relationship between temperature changes and the rate of chemical reaction, we investigate the temperature and concentration of particles around a vessel in the three different places. We describe three chemical components, A, B and C, which react and diffuse, and a temperature, which is affected by the reactions Fig. 2.

- I) A combines with B to form C, liberating heat.
- II) C decomposes to A and B, absorbing heat. The decomposition rate is temperature dependent.

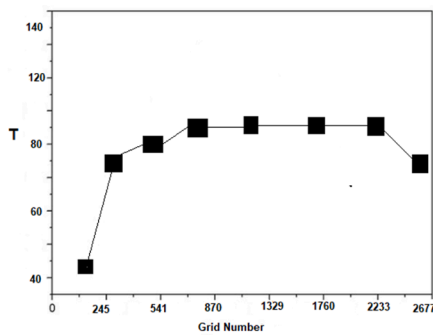
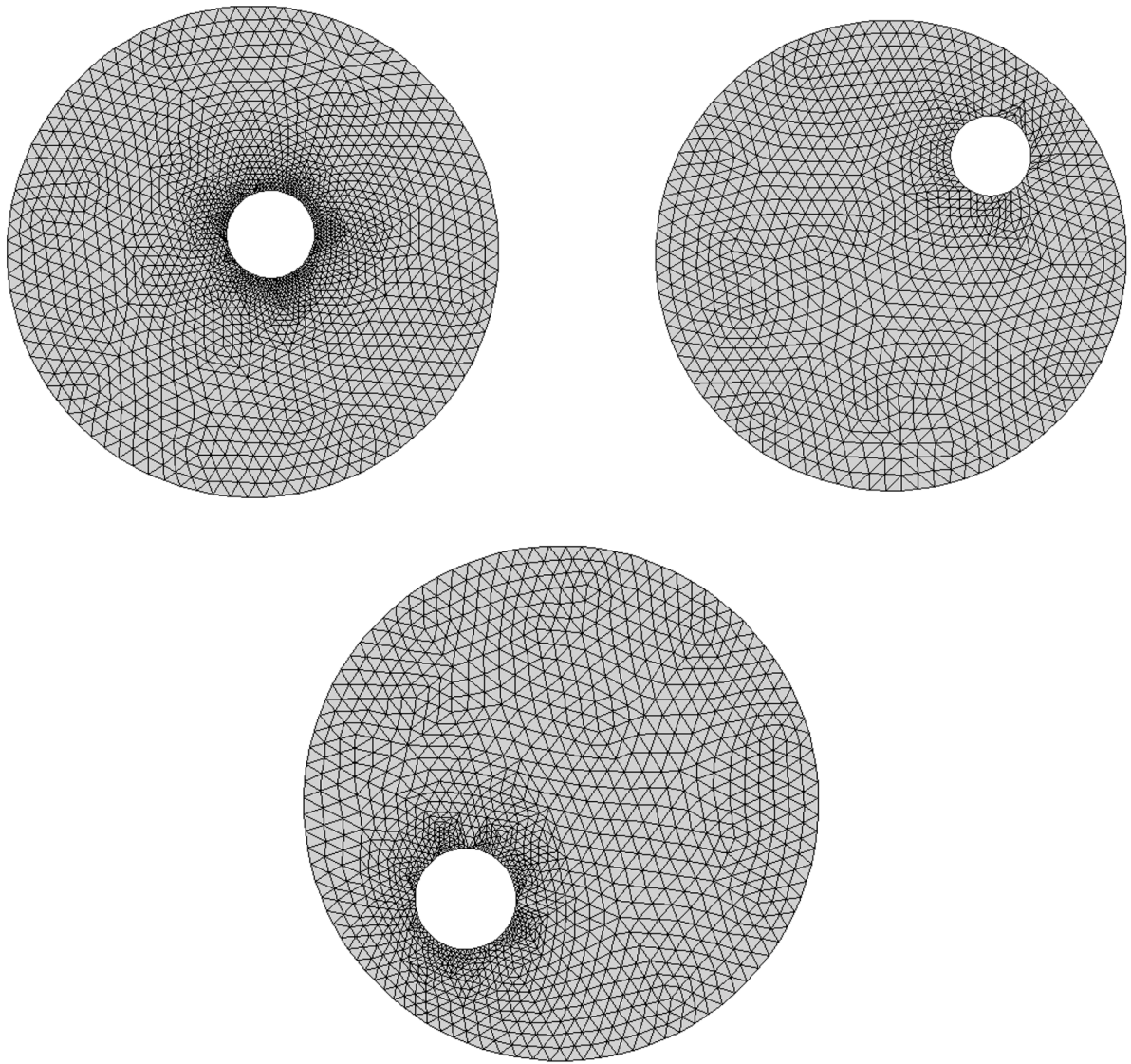
- III) A, B, C and Temperature diffuse with differing diffusion constants.

The boundary of the vessel is held cold, and heat is applied to a circular exclusion patch near the center, intended to model an immersion heater. What is an Immersion Heater? The simple answer is that it may be a device that gives hot water for your house and is fueled by electricity. The immersion water heater is partitioned from your central warming boiler or radiators, which means that, even if you're central warming fails, you should still be able to have warm water in your house .A, B and C cannot diffuse out the boundary. This example shows the application of FlexPDE to the solution of reaction-diffusion problems. The complete equations including the Arrhenius terms that describe the system are [21]:

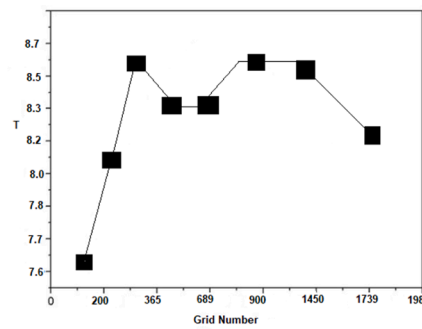
$$Kt \left( \frac{\partial^2 T \rightarrow}{\partial x^2} i + \frac{\partial^2 T \rightarrow}{\partial y^2} j + \frac{\partial^2 T \rightarrow}{\partial z^2} k \right) + Q + K1.e \left( -H1/(T+273) \right). (0.0025).A.B - K2.e \left( -H2/(T+273) \right). (0.0025).C.(T+273) = 0 \quad (1)$$

$$Ka. \left( \frac{\partial^2 A \rightarrow}{\partial x^2} i + \frac{\partial^2 A \rightarrow}{\partial y^2} j + \frac{\partial^2 A \rightarrow}{\partial z^2} k \right) - K1.e \left( -H1/(T+273) \right).A.B + K2.e \left( -H2/(T+273) \right).C.(T+273) = 0 \quad (2)$$

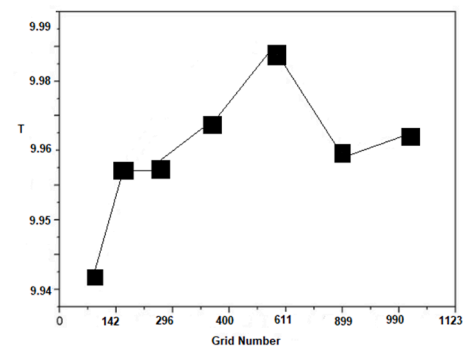
$$Kb \left( \frac{\partial^2 B \rightarrow}{\partial x^2} i + \frac{\partial^2 B \rightarrow}{\partial y^2} j + \frac{\partial^2 B \rightarrow}{\partial z^2} k \right) - K1.e \left( -\frac{H1}{T+273} \right).A.B + K2.e \left( -H2/(T+273) \right).C.(T+273) = 0 \quad (3)$$



a) Grid independent test for temperature around the center of vessel



b) Grid independent test for temperature around the vessel in the bottom



c) Grid independent test for temperature around the vessel in the top

Fig 3. Geometry of the mesh and grid independent test.

$$K_c \cdot \left( \frac{\partial^2 c \rightarrow}{\partial x^2} i + \frac{\partial^2 c \rightarrow}{\partial y^2} j + \frac{\partial^2 c \rightarrow}{\partial z^2} k \right) + K_1 \cdot e^{-H_1/(T+273)} \cdot A \cdot B - K_2 \cdot e^{-H_2/(T+273)} \cdot C \cdot (T + 273) = 0 \tag{4}$$

Where  $K_t$ ,  $K_a$ ,  $K_b$  and  $K_c$  are the diffusion constants, EABS is the heat liberated when A and B combine, and Q is any internal heat source. A, B,

C are the chemical component, T is the temperature parameter,  $H_1$  and  $H_2$  are the activation energy parameter for A + B and C species.  $K_1$  is the Reaction coefficient for A + B;  $K_2$  is the Reaction coefficient for C. The above equations include an energy equation and three equations related to chemical reactions of particles. In all the equations, a thermal energy storage source has been used, and radiation coefficients have also been calculated for the reactant and product streams. According to the terms

**Table 1**

Comparison of temperature for present work and Ebermann work [21] at  $K_1=0.05$ ,  $H_1=10$ ,  $K_1=1$ .

	$x = -1.5$	$x = -1$	$x = 0$	$x = 0.5$	$x = 0.75$	$x = 1$
Present work	0	26	50	68.98	80	100
Ebermann [21]	0	25.88	49.87	66.90	80	100

used in the above differential equations, the radiation parameters and the heat storage source significantly affect the behavior of the material particles involved in the chemical reaction and cause a change in their movement. Heat is transferred from the inner plate's boundaries to the boundary layers outside.

The boundary layer is : in the  $(0, -1) \rightarrow T = 0, a' = 0, b' = 0, c' = 0$  (5)

In the  $(-0.2, 0) \rightarrow T = 100, a' = 0, b' = 0, c' = 0$  (6)

Notice that the system is non-linear, as it contains terms involving A, B and C.Temp.

There are an infinite number of solutions to these equations, differing only in the total particle count. In reality, since particles are conserved, the final solution is uniquely determined by the initial conditions. But this fact is not embodied in the steady-state equations. The only way to impose this condition on the steady-state system is through an integral constraint equation, which describes the conservation of total particle number.

The images above (Fig. 3) show a triangular mesh around the vessels in different places. In the border areas around the inner vessel, the number of triangular grids is more and the distance between the boundaries of the grid is closer to each other, and the closer we get to the outer vessel from the edge of the boundaries, the lower the density of the grids. In areas where the lattice density is higher, changes in the concentration and temperature of the materials involved in the chemical reaction are greater. In according to grid independent test of mesh for regions that vessels are, the maximum grid number has been observed around the plate in the center and it has been shown that with the increase in the temperature of the reactant particles, the number of elements and networks has increased.

### 3. Methodology

#### 3.1. Finite element method (FEM) and RSM method

The finite element method (abbreviated as FEM) is a numerical method for obtaining a hypothetical solution to a set of problems managed by elliptic partial differential equations. Such problems are called boundary problems because they involve a partial differential equation. (FEM) is an extremely valuable device in the field of graceful construction of complex numerically approximate physical structures such as for standard exposure arrangements. In statistics, response surface methodology (RSM) examines the relationship between some exemplary variables and one or more response variables. This method was developed by George E.P.Box and K.B. Wilson in 1951. The main idea of RSM is to use a series of planned experiments to get the best answer. Box and Wilson recommend using a quadratic polynomial model for this. They recognize that this model is just an approximation, but they use it because it is easy to evaluate and apply even if little is known about its preparation. The benefits of using this technique include high adaptability, high accuracy, time-dependent simulation, and improved visualization of the studied shape's boundaries. Other numerical models, such as ADM and HPM, can produce similar results, but they lack the application of this method.

#### 3.2. Validation for methods

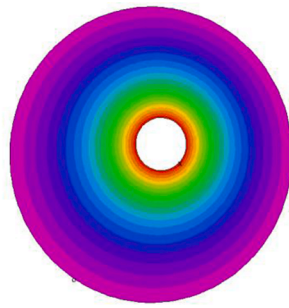
In this section, for validation, we compared our work by Ebermann

et al. [21]. The amount of computational error in our work is very low compared to Ebermann work. The maximum number of errors happened in  $x = 0.5$  and minimum number of errors happened in  $x = 1$ . Table 1 shows the degree of convergence of a thermal parameter of the temperature of chemical reactions in different intervals. According to it, with the increasing distance from the center of the vessel to the outside, the temperature value in both studies has an upward trend and the results are close to each other.

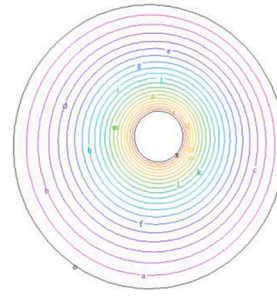
### 4. Discussions

The set of pictures above shows the temperature changes of the substances involved in the chemical reaction in different places of the inner vessel relative to each other. These modes are considered about the addition of a heat source with different heat degrees and without a heat source. Fig. 4 (a) to (f) show the temperature changes around the vessel fixed in the center of the larger vessel in different heat sources. According to the temperature lines shown around the inner vessel, we come to the conclusion that the more heat transfer from an external heat source to the center (similar to an immersion heater), the greater the distance between the reactant molecules and the more heat. It is released from the reaction of substances (a) and (b), and larger thermal vortices with negative pressure are formed behind the vessel. By reducing the amount of heat transfer to the center, less heat spreads around and the thermal boundary layer is smaller than the velocity boundary layer. As the heat transfer to the center increases, a large thermal boundary layer forms around the inner plate. This is a heat-generating process in the particles of the reacting material that is accompanied by the release of this received heat outside the inner container. It is suggested that this is a process. According to the science of fluids and thermodynamics, in this situation, the system's entropy increases, and the enthalpy becomes negative. Figs. 4 (g) to (r) show the temperature changes around the vessel fixed in the bottom of the larger vessel and top of the large vessel in different heat sources. Here too, by adding a heat source to the center of the vessel shape, the thermal boundary layer becomes thicker and transfers more heat to the surroundings. The heat flux lines also move away from each other with the addition of a heat source, and this indicates an increase in the intermolecular distance of the reactants. According to figs. 4 (q) and (r), considering that high heat transfer is given to the center, but behind the inner vessel, a large wake flow with a large negative pressure is formed, which prevents heat from passing around. In these cases, the temperature of the system increases, in fact, the heat created in the environment is released, which results in a negative value of heat of reaction. Therefore, we conclude that the best mode for increasing heat transfer from substances involved in a chemical reaction at the boundaries of the inner vessel occurs when the inner vessel is at the lowest point of the larger vessel in mode Heat source =5.

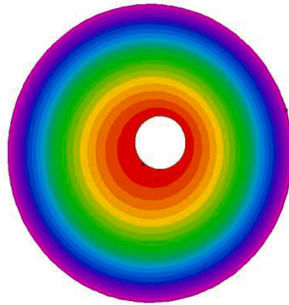
The set of pictures above shows the concentration changes of the substances involved in the chemical reaction in different places of the inner vessel relative to each other. These modes are considered about the addition of a heat source with different heat degrees and without a heat source. Figures a to f show the concentration changes around the vessel fixed in the center of the larger vessel in different heat sources. Considering that the temperature of the reacting substance (here a) has a direct relationship with the concentration, with the addition of temperature and heat transfer to the center of the vessel shape, the concentration of the substance also increases, and the closer we get to the outside of the center, the concentration of substance decreases. The concentration of the reactant also has a direct relationship with the temperature and heat transfer from the system. As the reactant's concentration increases, the reaction's temperature increases, and more energy are released. As the heat transfer to the center increases, a large thermal boundary layer forms around the inner vessel. This is a heat-generating process in the particles of the reacting material that is accompanied by the release of this received heat outside the inner container. It is suggested that this is a process. According to the science



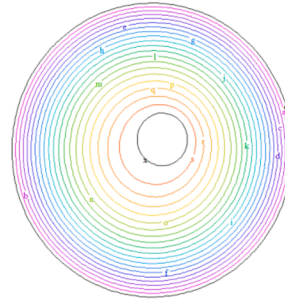
a) Temperature profile around the vessel in the center for heat source=0



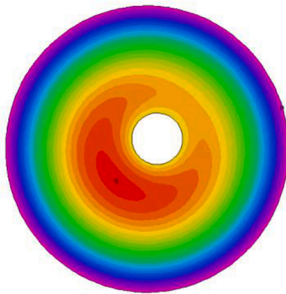
b) Stream line of Temperature profile around the vessel in the center for heat source=0



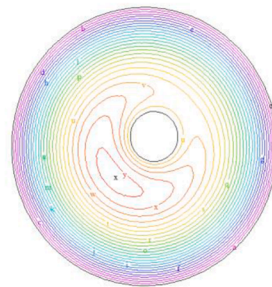
c) Temperature profile around the vessel in the center for heat source=3



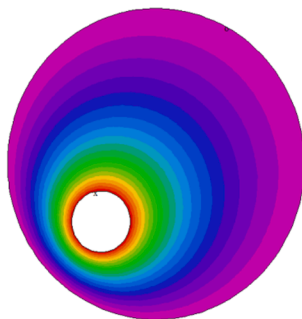
d) Stream line of Temperature profile around the vessel in the center for heat source=3



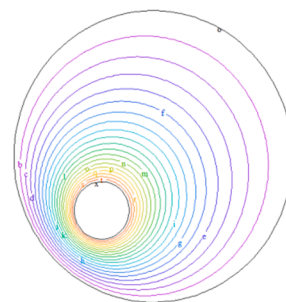
e) Temperature profile around the vessel in the center for heat source=5



f) Stream line of Temperature profile around the vessel in the center for heat source=5



g) Temperature profile around the vessel in the bottom for heat source=0



h) Stream line of Temperature profile around the vessel in the bottom for heat source=0

Fig 4. Temperature changes across the vessel for exceptional values of warmth source.

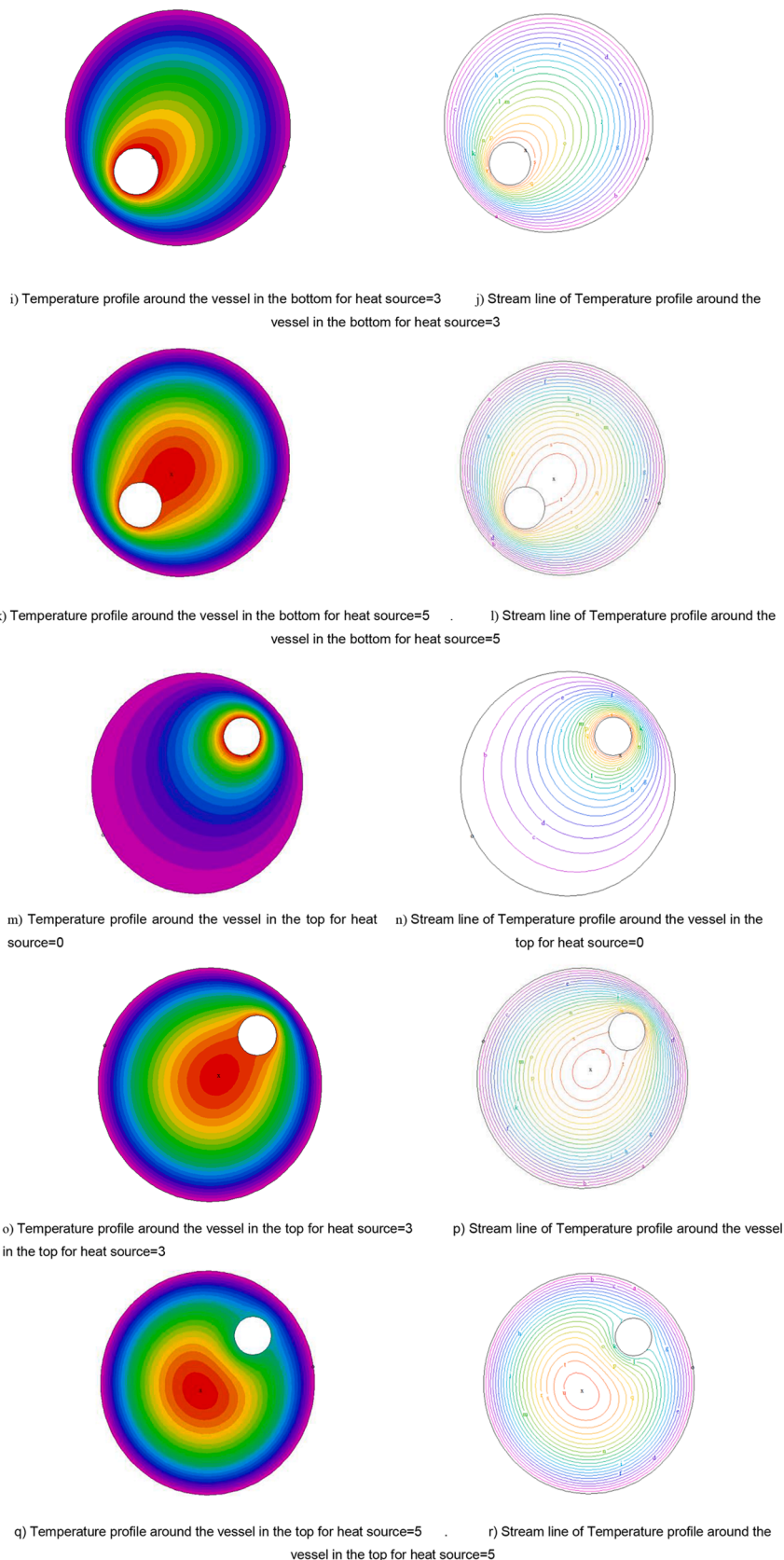
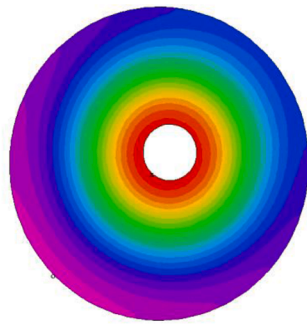


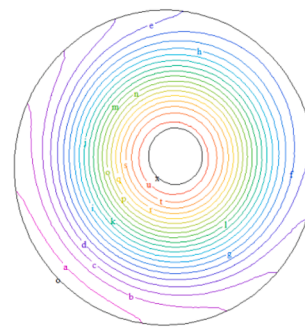
Fig 4. (continued).

of fluids and thermodynamics, in this situation, the system's entropy increases, and the enthalpy becomes negative. Fig. 4 (g-a) to (r-a) show the concentration changes around the vessel fixed in the bottom of the

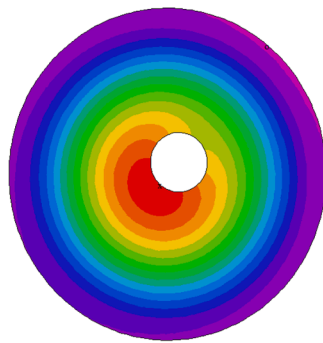
larger vessel and top of the large vessel in different heat sources. According to figs. 4 (g-a) and (h-a), when there is no heat source, the concentration of the reactant (a) is spread uniformly on all the borders of



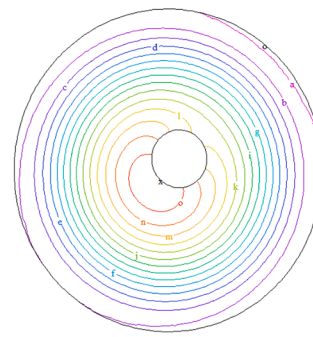
a) Concentration profile of component (a) around the vessel in the center for heat source=0



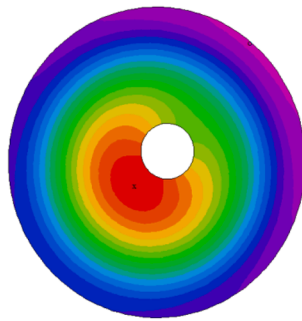
b) Stream line of concentration profile of component (a) around the vessel for heat source=0



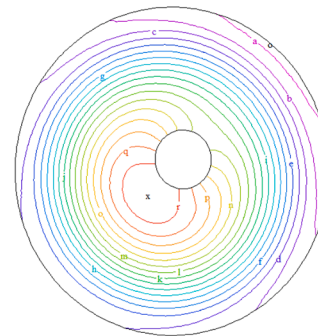
c) Concentration profile of component (a) around the vessel in the center for heat source=3



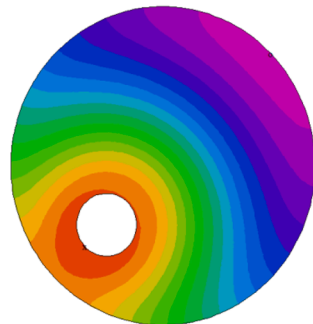
d) Stream line of concentration profile of component (a) around the vessel for heat source=3



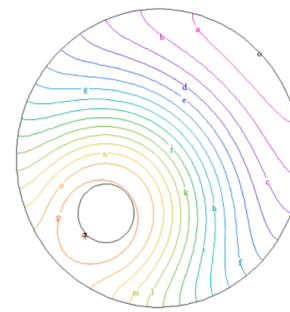
e) Concentration profile of component (a) around the vessel in the center for heat source=5



f) Stream line of concentration profile of component (a) around the vessel for heat source=5



g) Concentration profile of component (a) around the vessel in the bottom for heat source=0



h) Stream line of concentration profile of component (a) around the vessel for heat source=0

Fig 4-a. Concentration alterations around the vessel for different values of heat source for component (a).

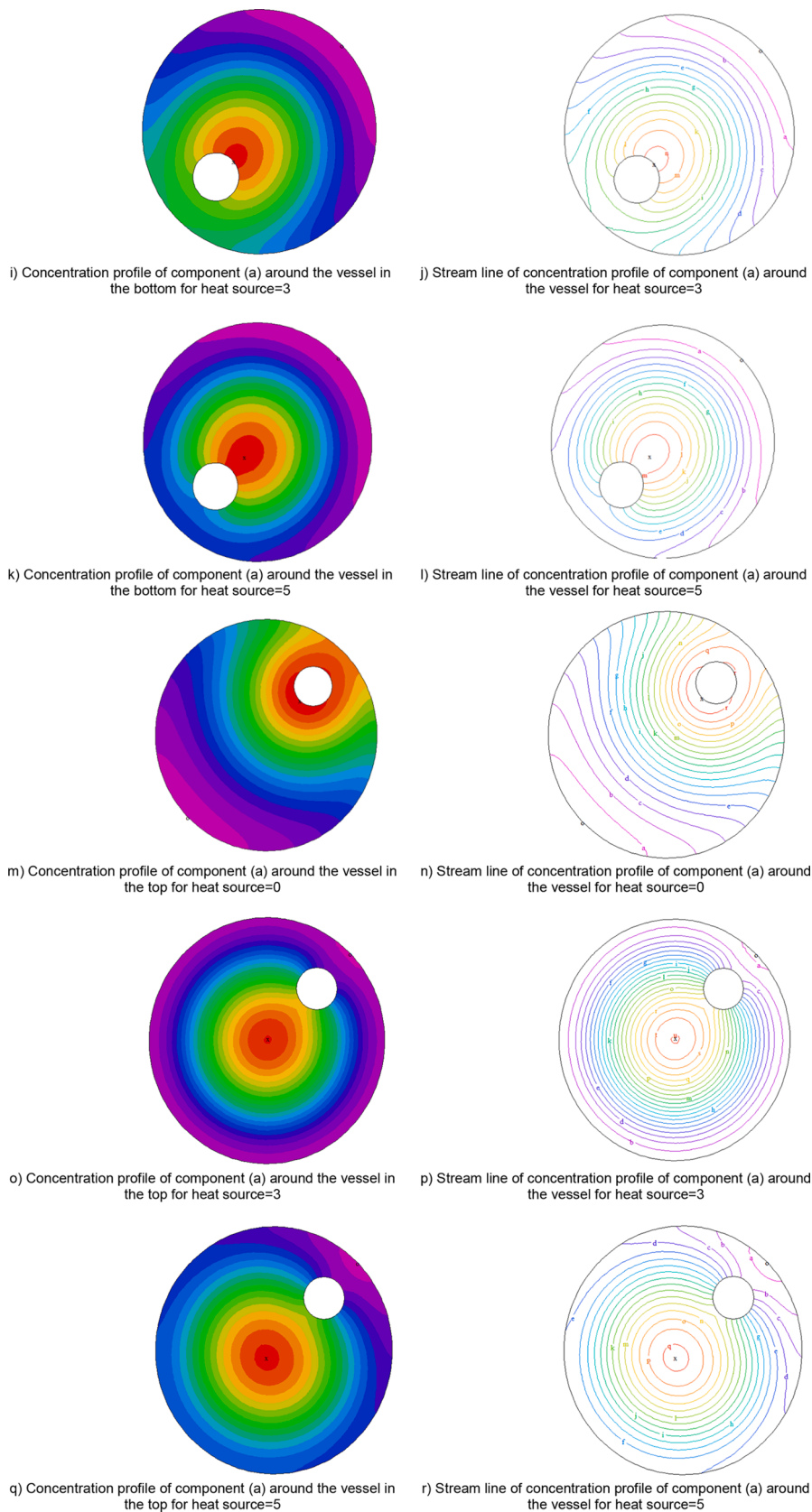
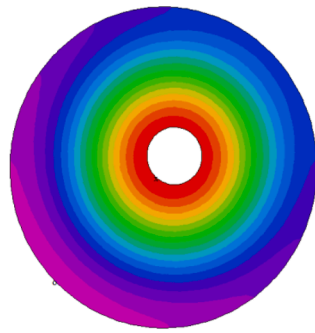


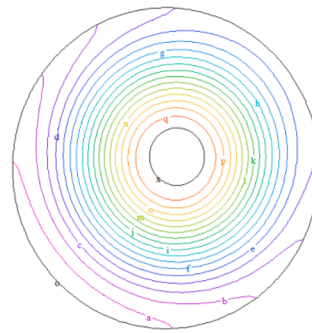
Fig 4-a. (continued).

the inner vessel with the maximum viscosity, and the back of the object is denser than the front, but with Adding and intensifying the heat transfer to the center of the vessel, the concentration of reactant

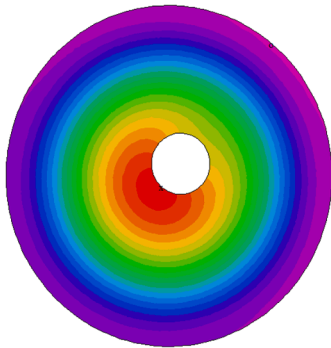
substance (a) is reduced at the back of the object, and as we increase the temperature, this concentration is formed with a wider range and larger amounts in front of the vessel. According to Fig. 4 m-4-a and n-4-a, the



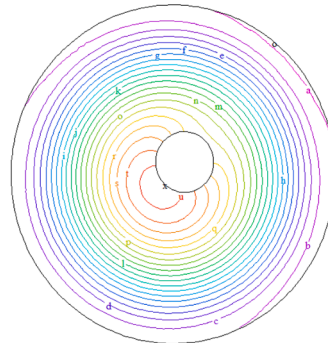
a) Concentration profile around the vessel in the center for heat source=0 for component (b)



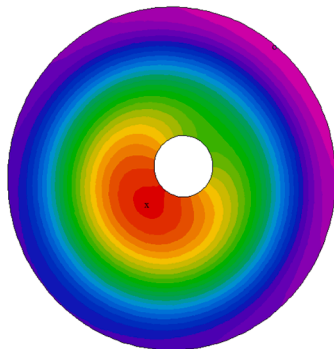
b) Stream line of concentration profile around the vessel for heat source=0 for component (b)



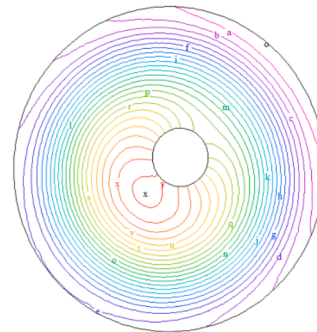
c) Concentration profile around the vessel in the center for heat source=3 for component (b)



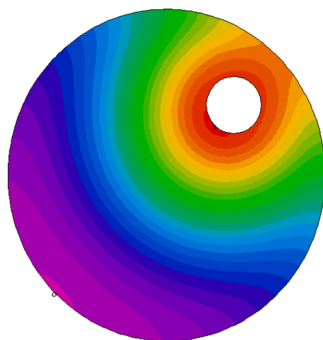
d) Stream line of concentration profile around the vessel for heat source=3 for component (b)



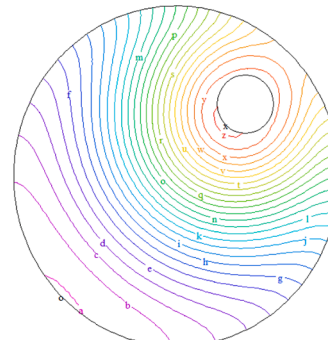
e) Concentration profile around the vessel in the center for heat source=5 for component (b)



f) Stream line of concentration profile around the vessel for heat source=5 for component (b)



g) Concentration profile around the vessel in the top for heat source=0 for component (b)



h) Stream line of concentration profile around the vessel for heat source=0 for component (b)

**Fig 4-b.** Concentration alterations around the vessel for different values of heat source for component (b).

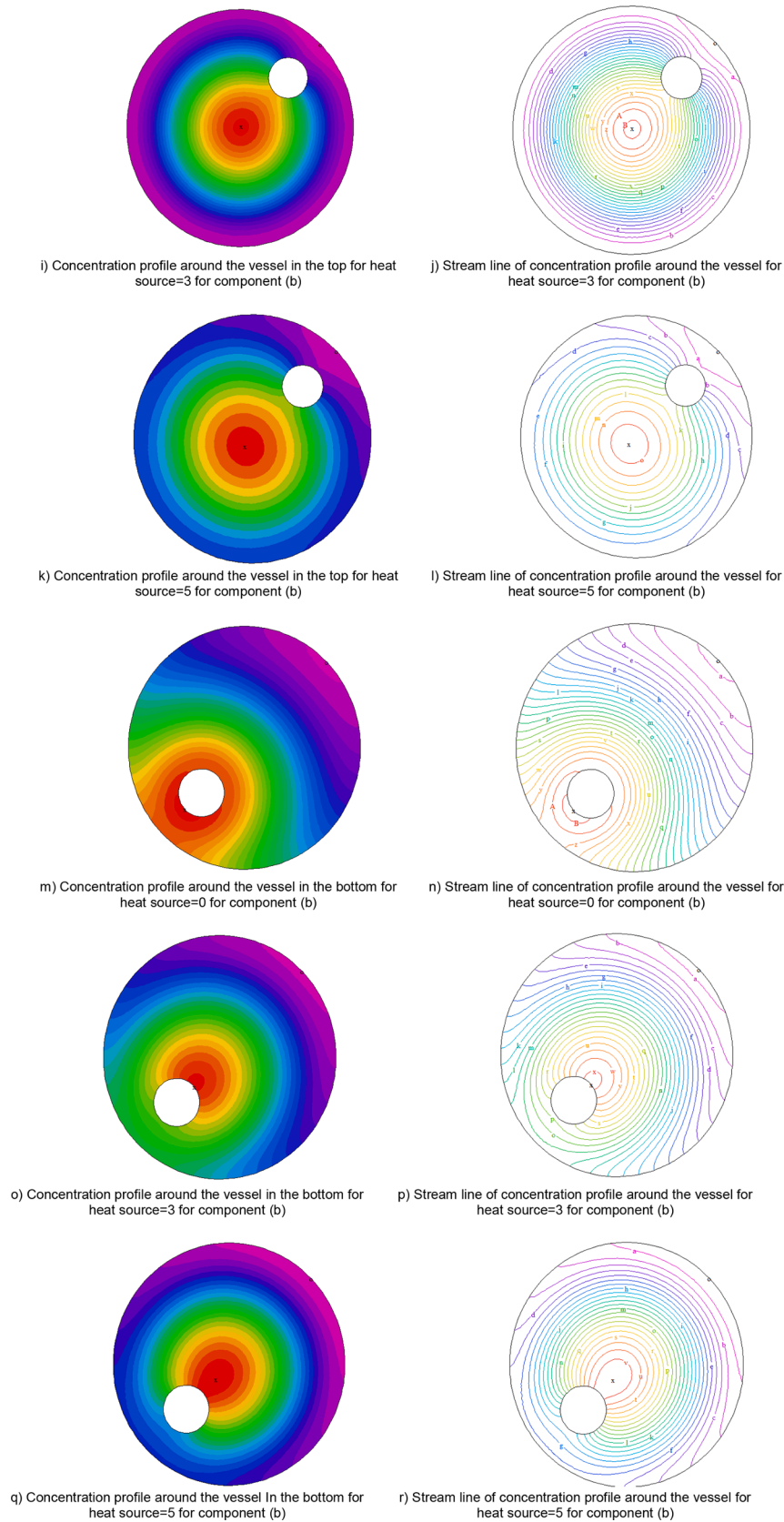
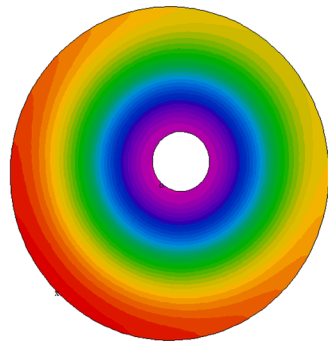


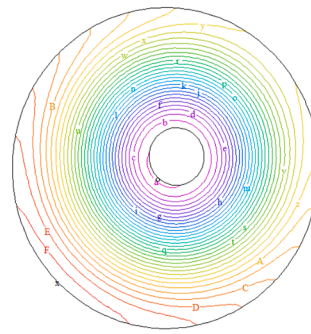
Fig 4-b. (continued).

concentration line of substance a is compressed around the borders of the inner vessel and has a high viscosity, and the concentration value decreases as it moves away from the center, and substance (a) is viscous

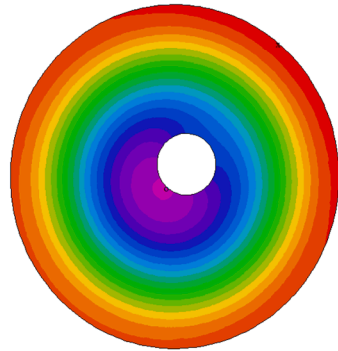
Loses. These reactions cause changes in the energy level, and therefore enthalpy changes occur. The system defines and calculates these enthalpy changes, and the environment has no role. According to the



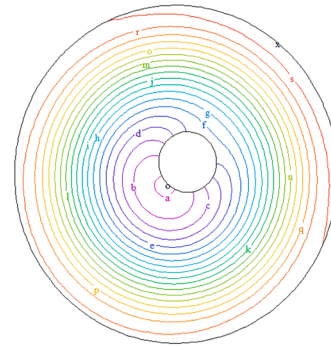
a) Concentration profile around the vessel in the center for heat source=0 for component (c)



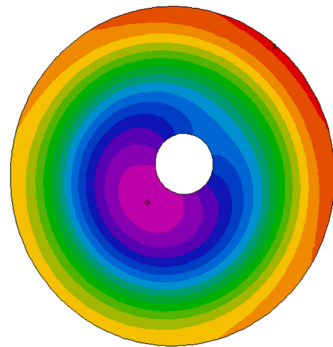
b) Stream line of concentration profile around the vessel for heat source=0 for component (c)



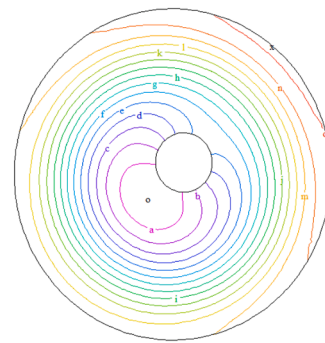
c) Concentration profile around the vessel in the center for heat source=3 for component (c)



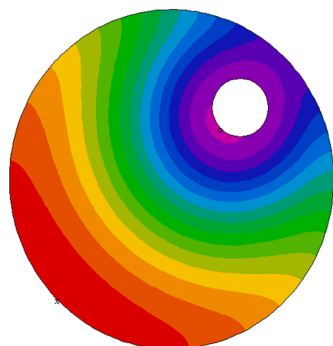
d) Stream line of concentration profile around the vessel for heat source=3 for component (c)



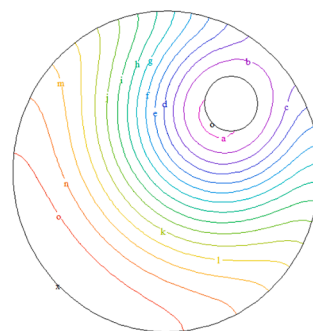
e) Concentration profile around the vessel in the center for heat source=5 for component (c)



f) Stream line of concentration profile around the vessel for heat source=5 for component (c)



g) Concentration profile around the vessel in the top for heat source=0 for component (c)



h) Stream line of concentration profile around the vessel for heat source=0 for component (c)

Fig 4-c. Concentration alterations around the vessel for different values of heat source for component (c).

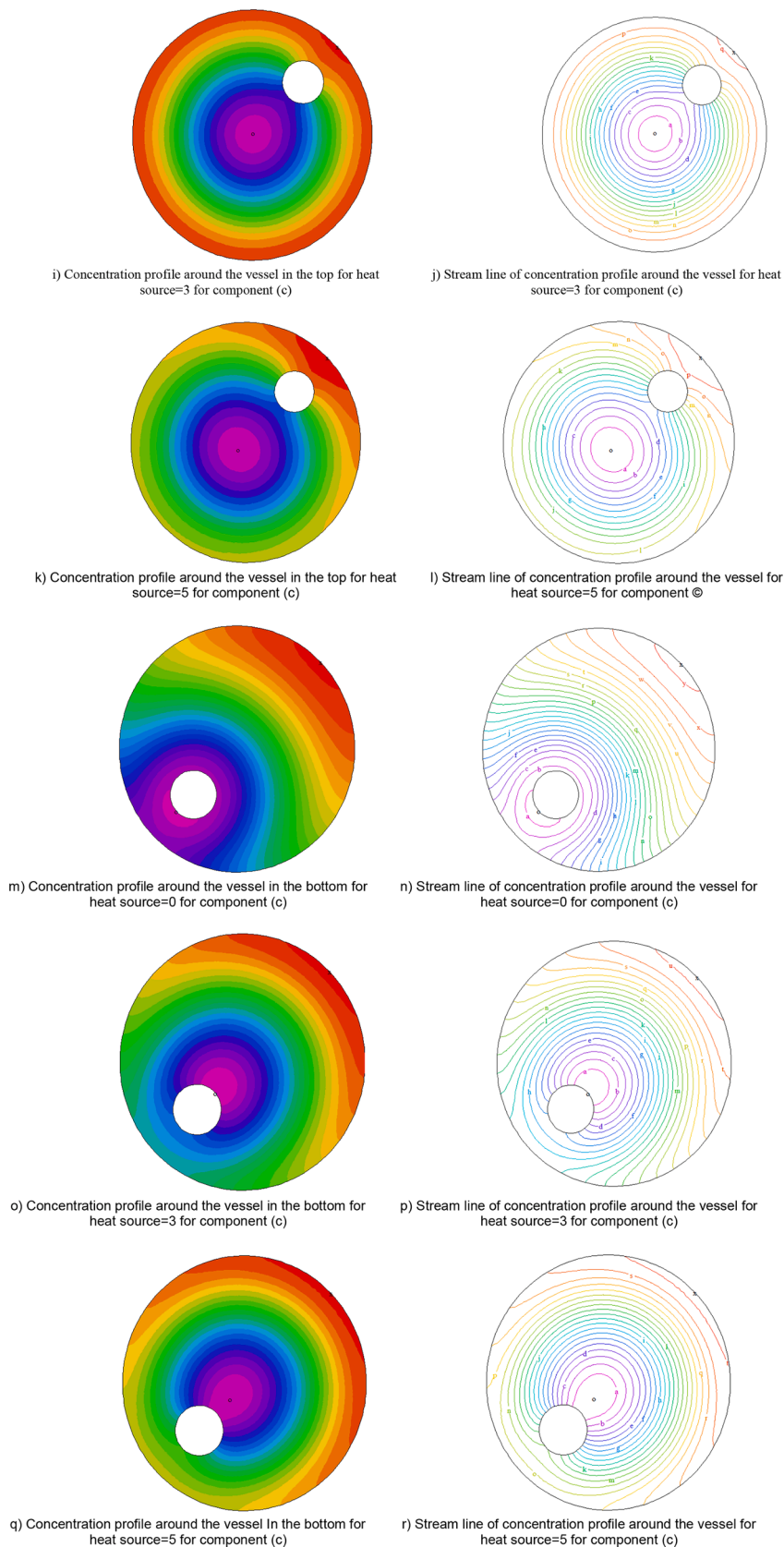
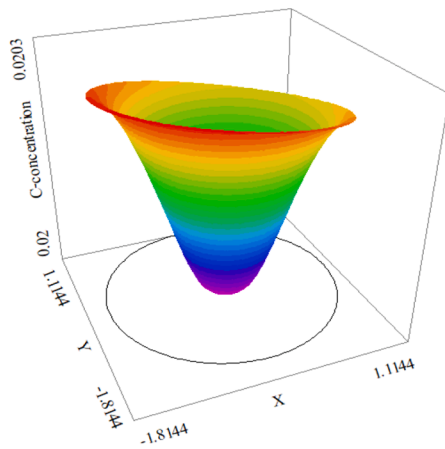


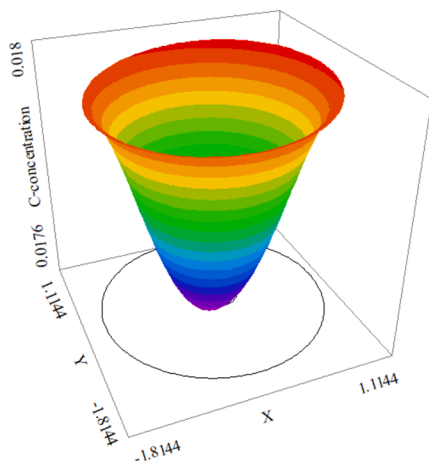
Fig 4-c. (continued).

system, as heat is released from the boundary layer of the inner container, the enthalpy value decreases and becomes negative. The concentration of the reactant also has a direct relationship with the

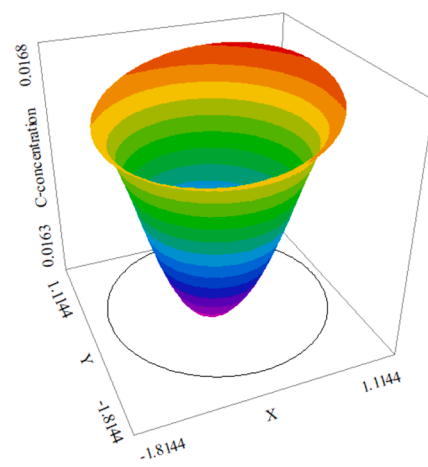
temperature and heat transfer from the system. As the reactant's concentration increases, the reaction's temperature increases, and more energy are released. By adding a heat source according to figures p-4-a



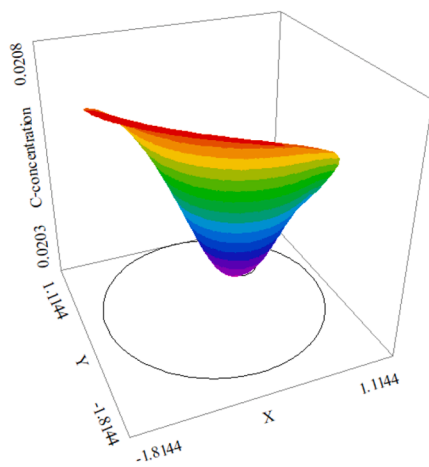
a) 3D concentration profile for component (c) near the vessel in the center by heat source=0



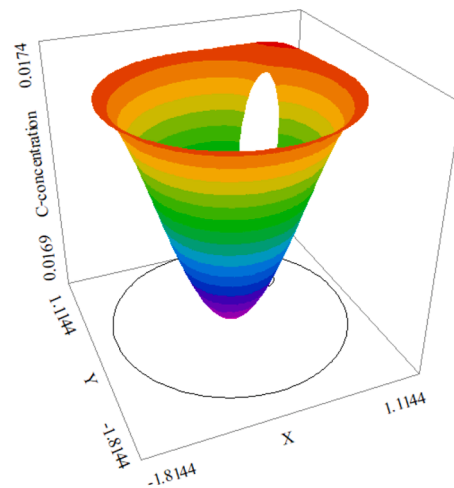
b) 3D concentration profile for component (c) near the vessel in the center by heat source=3



c) 3D concentration profile for component (c) near the vessel in the center by heat source=5.

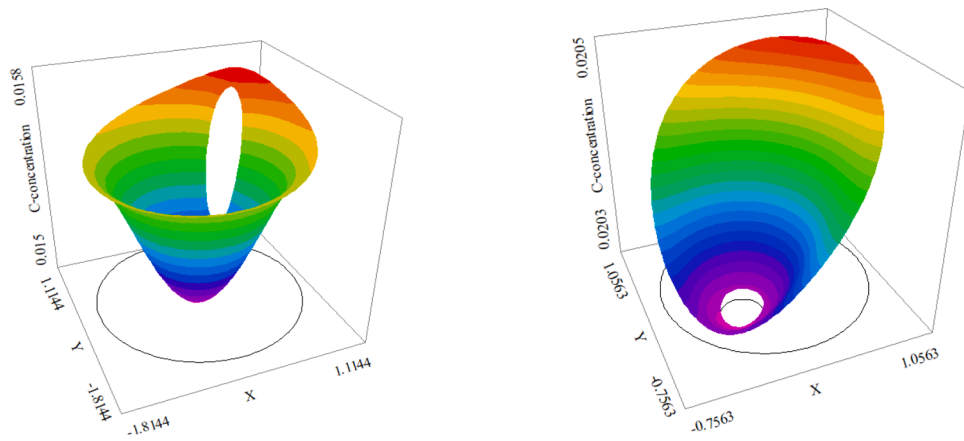


d) 3D concentration profile for component (c) near the vessel in the top by heat source=0

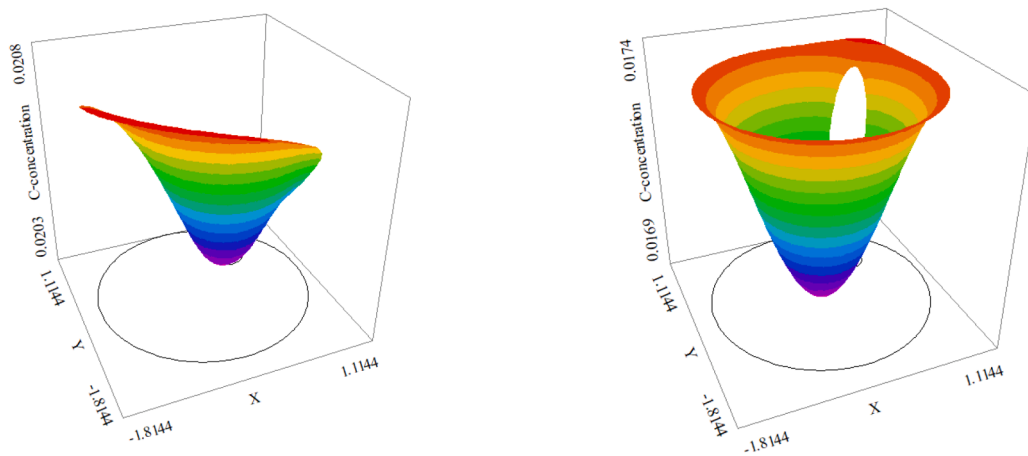


e) 3D concentration profile for component (c) near the vessel in the top by heat source=3.

Fig 4-d. Three-dimensional images concentration alterations around the vessel for component (c).



f) 3D concentration profile for component (c) near the vessel in the top by heat source=5 g) 3D concentration profile for component (c) near the vessel in the bottom by heat source=0



h) 3D concentration profile for component (c) near the vessel in the bottom by heat source=3 i) 3D concentration profile for component (c) near the vessel in the bottom by heat source=5.

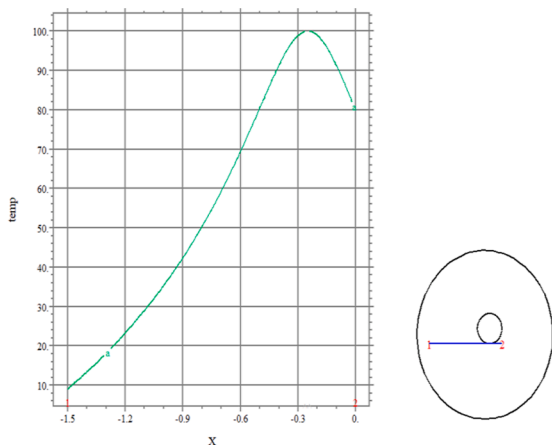
Fig 4-d. (continued).

to the end, the concentration of the reactant (a) is not high compared to the previous cases around the inner vessel, so the highest concentration occurs in the center of the larger vessel and around at the inner vessel boundaries, the reactant concentration values decrease. When the inner vessel is placed at the highest point of the larger vessel, the more heat is transferred to the surface of the inner vessel, the concentration of reactant decreases.

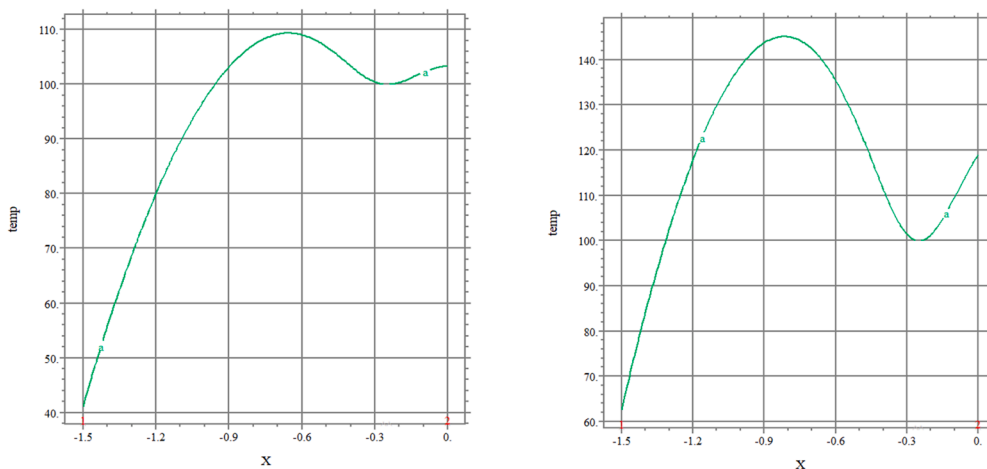
The set of pictures above shows the concentration changes of the substances involved in the chemical reaction in different places of the inner vessel relative to each other. These modes are considered about the addition of a heat source with different heat degrees and without a heat source. Figs. 4 (a-b) to (f-b) show the concentration changes for component (b) around the vessel fixed in the center of the larger vessel in different heat sources. Considering that the temperature of the reacting substance (here b) has a direct relationship with the concentration, with the addition of temperature and heat transfer to the center of the vessel shape, the concentration of the substance also increases, and the closer we get to the outside of the center, the concentration of substance decreases. The concentration of the reactant also has a direct relationship with the temperature and heat transfer from the system. As the reactant's concentration increases, the reaction's temperature increases, and more energy are released. According to figs. 4 (g-b) to (l-b), the concentration line of substance (b) is compressed around the borders of the inner vessel and has a high viscosity, and the concentration value

decreases as it moves away from the center, and substance (b) is viscous. By adding a heat source according to figures k-6 to the end, the concentration of the reactant (b) is not high compared to the previous cases around the inner vessel, so the highest concentration occurs in the center of the larger vessel and around at the inner vessel boundaries, the reactant concentration values decrease. When the inner vessel is placed at the highest point of the larger vessel, the more heat is transferred to the surface of the inner. Figs. 4 (m-b) to (r-b) show the concentration changes around the vessel fixed in the bottom of the larger vessel in different heat sources. According to Fig. 4 m-(4-b) and n-(4-b), when there is no heat source, the concentration of the reactant (b) is spread uniformly on all the borders of the inner vessel with the maximum viscosity, and the back of the object is denser than the front, but with Adding and intensifying the heat transfer to the center of the vessel, the concentration of reactant substance (b) is reduced at the back of the object, and as we increase the temperature, this concentration is formed with a wider range and larger amounts in front of the vessel.

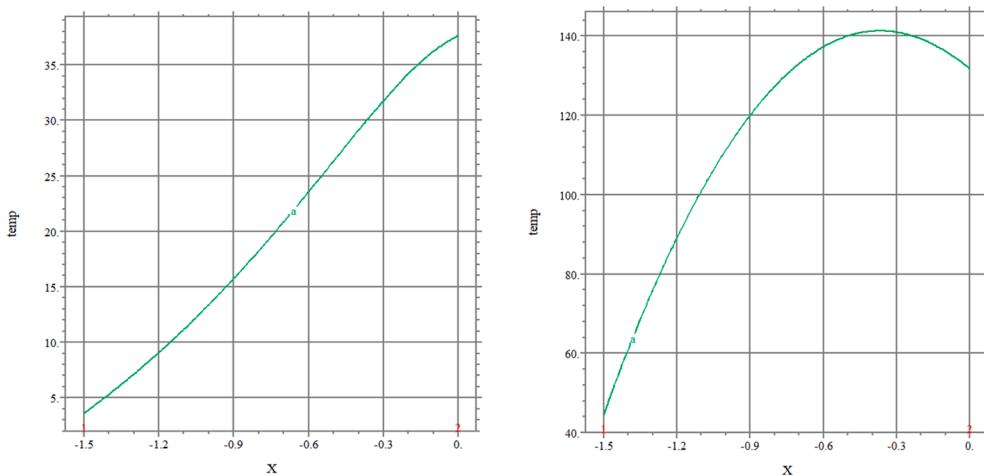
The set of pictures above shows the concentration changes of the substances involved in the chemical reaction in different places of the inner vessel relative to each other. These modes are considered about the addition of a heat source with different heat degrees and without a heat source. Figs. 4 (a-c) to (f-c) show the concentration changes for component (c) around the vessel fixed in the center of the larger vessel in different heat sources. Considering that substance (c) releases two other



a) Two dimensional graph of temperature changes in terms of distance from the center of the vessel to outside the environment for heat source=0

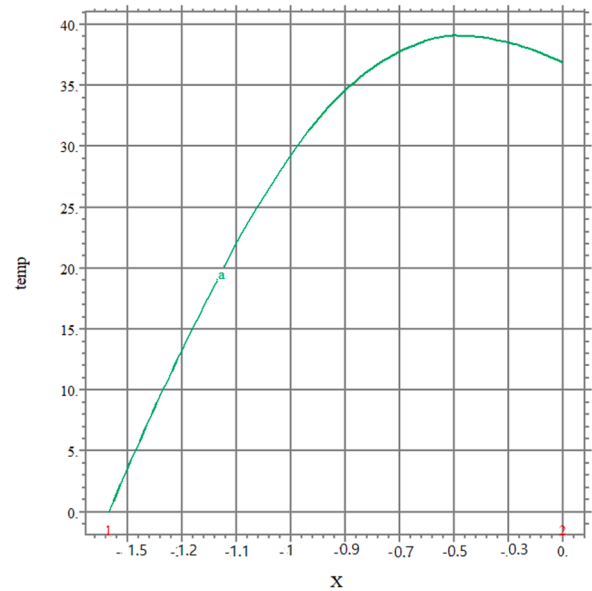
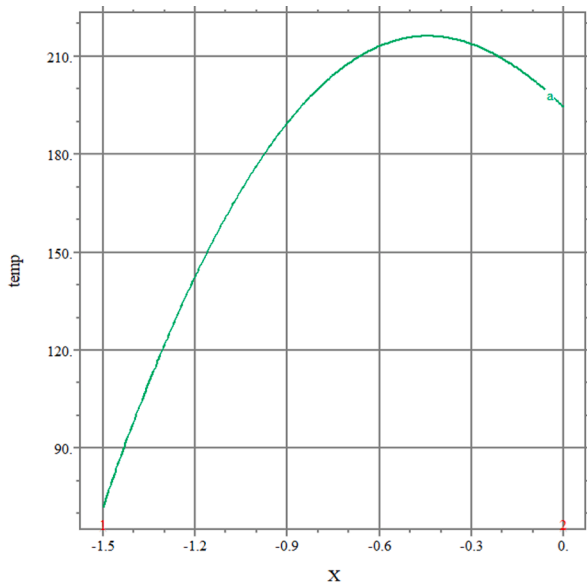


b) Two dimensional graph of temperature changes in terms of distance from the center of the vessel to outside the environment for heat source=3 c) Two dimensional graph of temperature changes in terms of distance from the center of the vessel to outside the environment for heat source=5

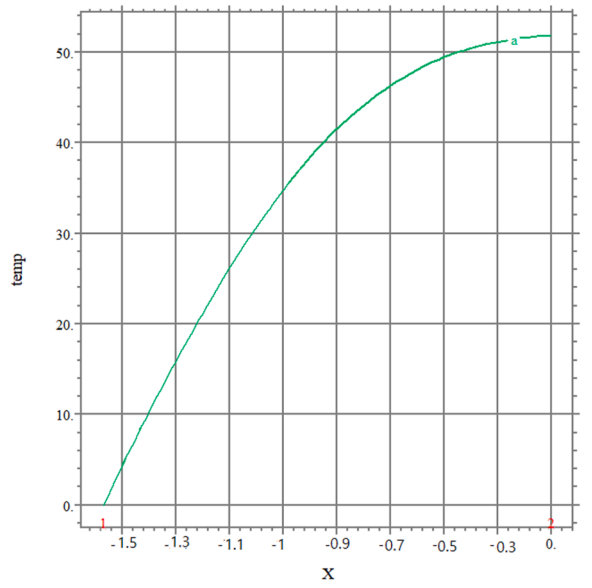
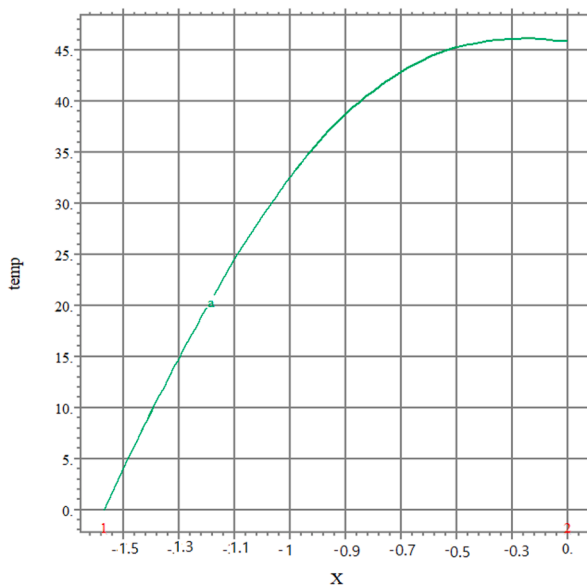


d) Two dimensional graph of temperature changes in terms of distance from the center of the top inner vessel to outside for heat source=0 e) d) Two dimensional graph of temperature changes in terms of distance from the center of the top inner vessel to outside for heat source=3

Fig 5. Temperature changes of reacting materials at certain intervals with different heat sources.



f) Two dimensional graph of temperature changes in terms of distance from the center of the top inner vessel to outside for heat source=5 g) Two dimensional graph of temperature changes in terms of distance from the center of the bottom inner vessel to outside for heat source=0

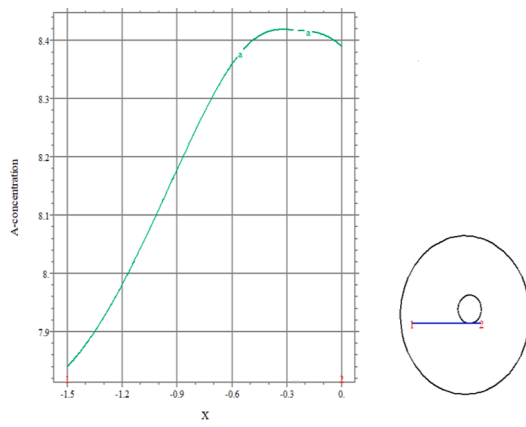


h) Two dimensional graph of temperature changes in terms of distance from the center of the bottom inner vessel to outside for heat source=3 i) Two dimensional graph of temperature changes in terms of distance from the center of the bottom inner vessel to outside for heat source=5

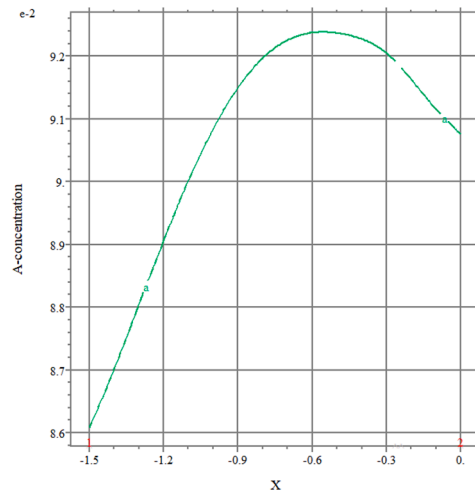
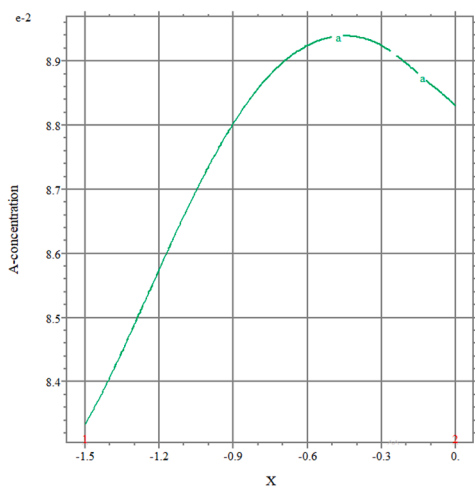
Fig 5. (continued).

reacting substances, i.e. substances (a) and (b), by absorbing heat, then with these interpretations and existing contours, we conclude that with the increase of heat applied to the center of the vessel without a heat source. Also, the concentration of substance (c) has an inverse relationship with the concentration of substances (a) and (b). According to the changes in the concentration of the produced substance (c), it can be seen that this process is endothermic. According to it, energy and heat are received and absorbed by substance (c), and entropy decreases. According to figures g-(4-c) to l-(4-c), the concentration line of substance (c) is not compressed around the borders of the inner vessel and has a less viscosity, and the concentration value increases as it moves away from the center, and substance (c) is not viscous. According to the concentration lines of substance (c) (in figs. (h-c), (j-c), and l-(4-c),

we conclude that with the increase of heat transfer to the center of the inner vessel, the temperature around the borders of the vessel increases and the rate of diffusion of substance (c) and its decomposition is very high. Also, high-speed wake flows are formed in the front part of the inner vessel with large vortices, and the pressure of the reactant is reduced. Figs. 4 (m-c) to (r-c) show the concentration changes around the vessel fixed in the bottom of the larger vessel in different heat sources. In the case where the inner vessel is placed at the end of the larger vessel (lower part), with the increase of heat transfer to the inner center of the inner vessel, the concentration of the produced substance (c) behind the inner vessel increases from the minimum value to the maximum value, and the viscosity increases and the farther towards the area and moving around, the concentration of substance (c) decreases



a) Two dimensional graph of concentration changes of component (a) in terms of distance from the center of the vessel to outside the environment for heat source=0.



b) Two dimensional graph of concentration changes of component (a) in terms of distance from the center of the vessel to outside the environment for heat source=3.

c) Two dimensional graph of concentration changes of component (a) in terms of distance from the center of the vessel to outside the environment for heat source=5.

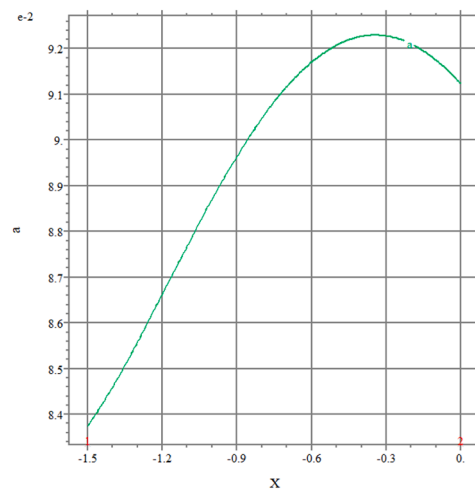
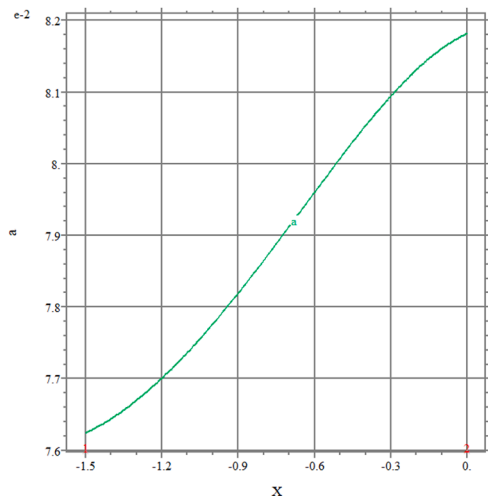
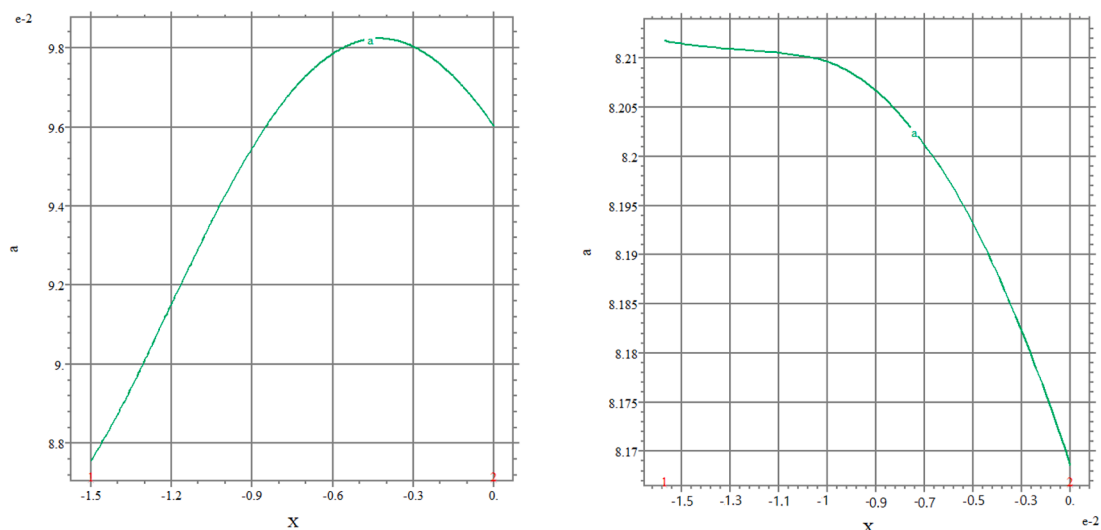


Fig 5-a. Concentration changes of reacting materials for component (a) at certain intervals with different heat sources.

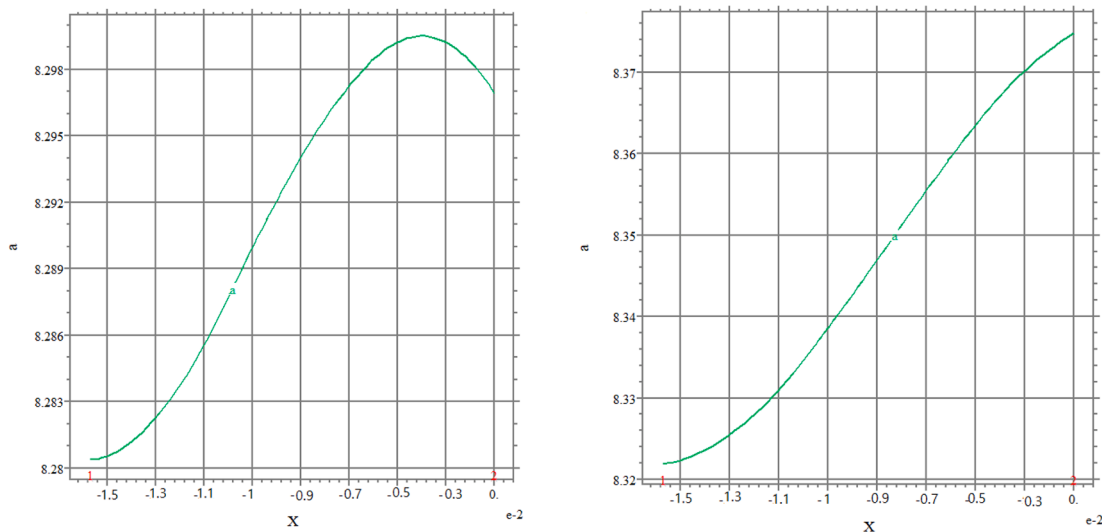
d) Two dimensional graph of concentration changes of component (a) in terms of distance from the top of the vessel to outside the environment for heat source=0.

e) Two dimensional graph of concentration changes of component (a) in terms of distance from the top of the vessel to outside the environment for heat source=3.



f) Two dimensional graph of concentration changes of component (a) in terms of distance from the top of the vessel to outside the environment for heat source=5.

g) Two dimensional graph of concentration changes of component (a) in terms of distance from the bottom of the vessel to outside the environment for heat source=0.



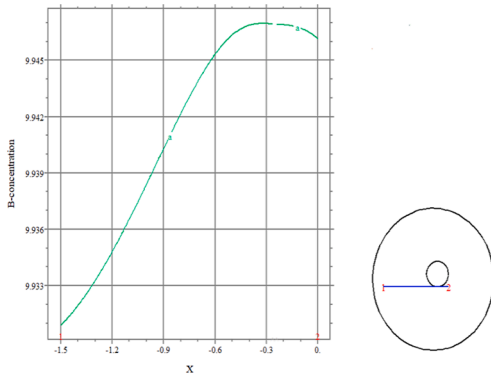
h) Two dimensional graph of concentration changes of component (a) in terms of distance from the bottom of the vessel to outside the environment for heat source=3.

i) Two dimensional graph of concentration changes of component (a) in terms of distance from the bottom of the vessel to outside the environment for heat source=5.

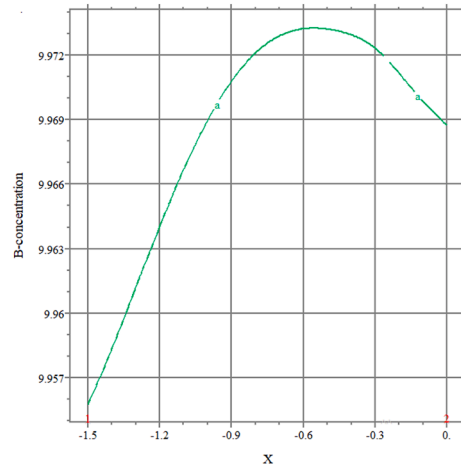
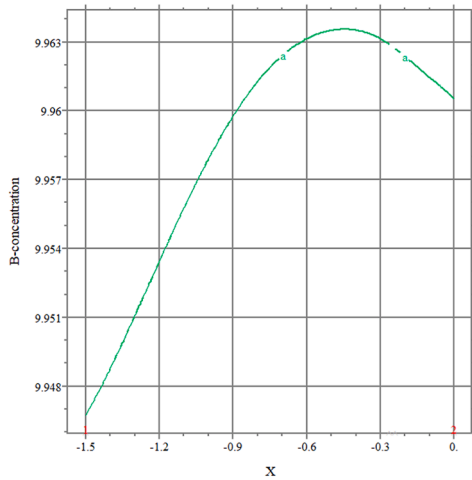
Fig 5-a. (continued).

and reaches its minimum value. A system of reactants that absorb heat from the environment in an endothermic reaction will have positive enthalpy changes. An endothermic reaction is associated with a decrease

in the temperature of a system. Finally, in an endothermic reaction, the heat of reaction will have a positive sign. The endothermic reaction cannot occur spontaneously but must be done on the work system for

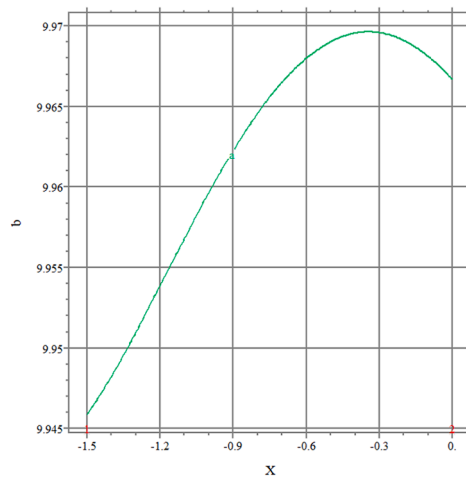
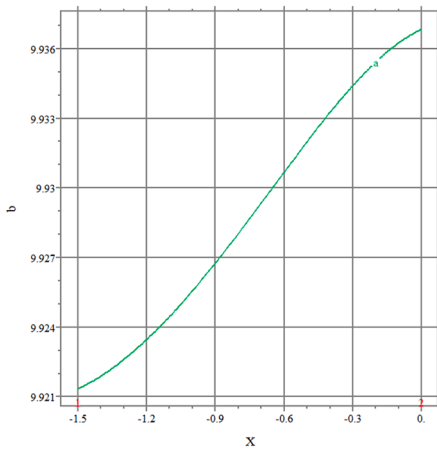


a) Two dimensional graph of concentration changes of component (b) in terms of distance from the center of the vessel to outside the environment for heat source=0.



b) Two dimensional graph of concentration changes of component (b) in terms of distance from the center of the vessel to outside the environment for heat source=3.

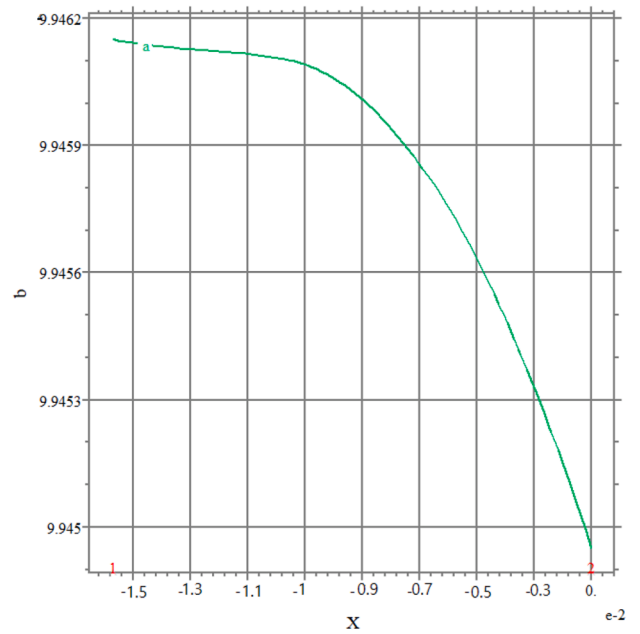
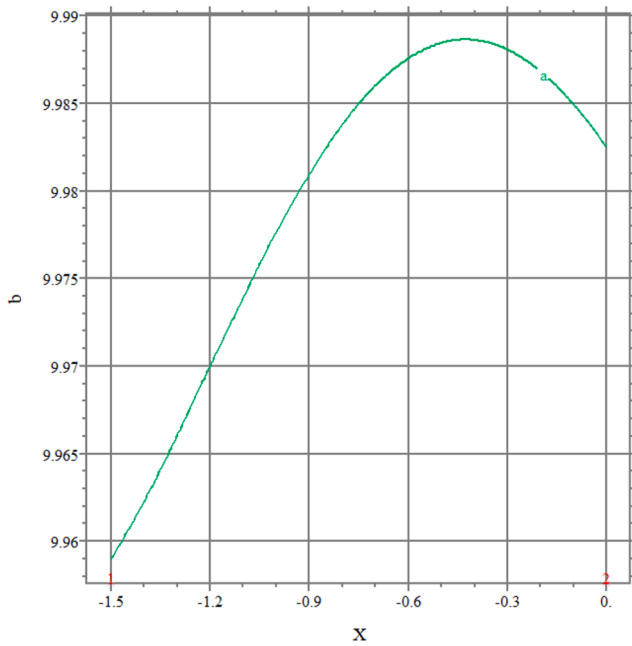
c) Two dimensional graph of concentration changes of component (b) in terms of distance from the center of the vessel to outside the environment for heat source=5.



d) Two dimensional graph of concentration changes of component (b) in terms of distance from the top of the vessel to outside the environment for heat source=0.

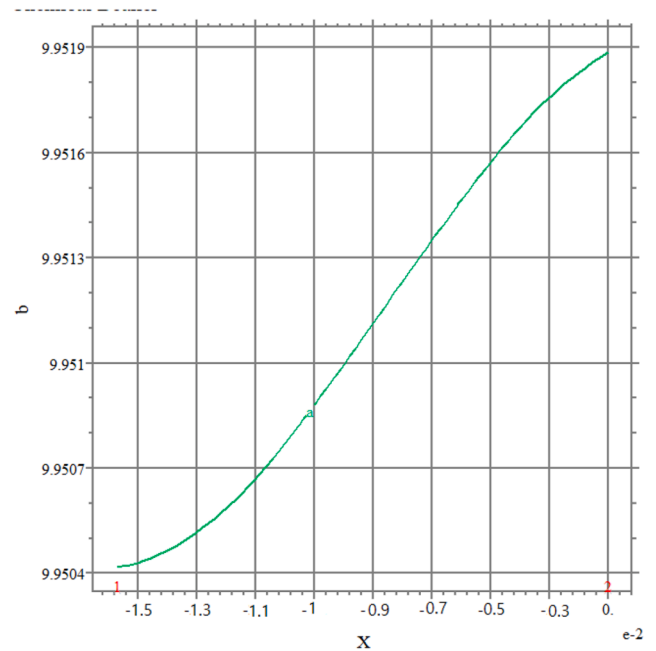
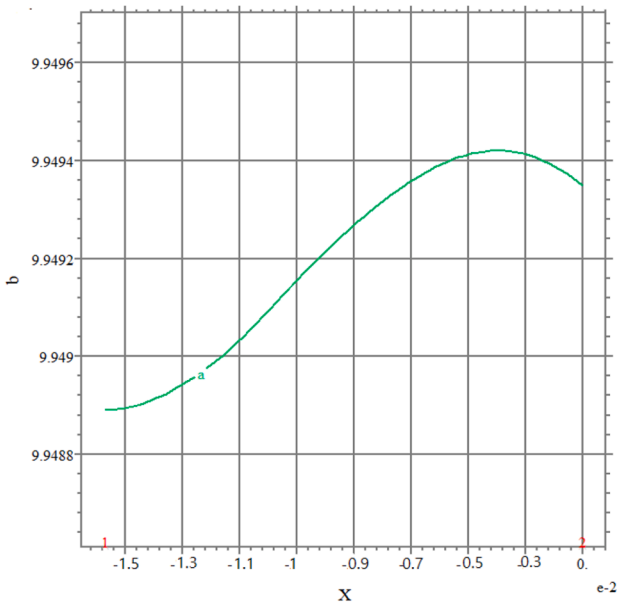
e) Two dimensional graph of concentration changes of component (b) in terms of distance from the top of the vessel to outside the environment for heat source=3.

**Fig 5-b.** Concentration changes of reacting materials for component (b) at certain intervals with different heat sources.



f ) Two dimensional graph of concentration changes of component (b) in terms of distance from the top of the vessel to outside the environment for heat source=5.

g) Two dimensional graph of concentration changes of component (b) in terms of distance from the bottom of the vessel to outside the environment for heat source=0.



h) Two dimensional graph of concentration changes of component (b) in terms of distance from the bottom of the vessel to outside the environment for heat source=3.

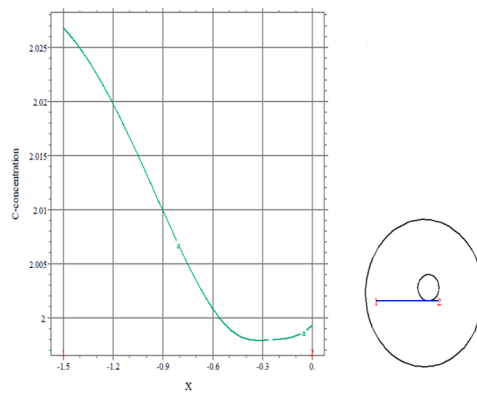
i) Two dimensional graph of concentration changes of component (b) in terms of distance from the bottom of the vessel to outside the environment for heat source=5.

Fig 5-b. (continued).

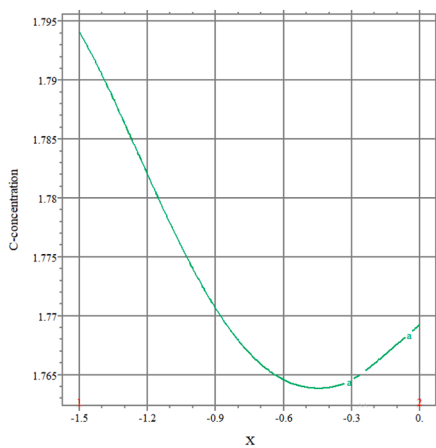
this type of reaction to progress. Of course, when the enthalpy and entropy changes are such that we have negative Gibbs free energy, these reactions also occur spontaneously. When an endothermic reaction absorbs energy, a temperature drop occurs during the response.

Endothermic reactions are identified by increased enthalpy (positive enthalpy changes) and a positive sign of energy.

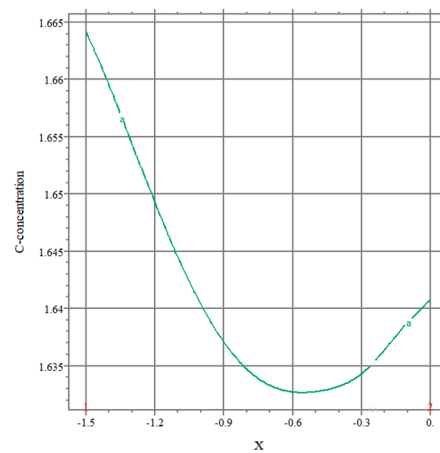
The set of pictures above shows the 3D concentration changes of the substances involved in the chemical reaction in different places of the



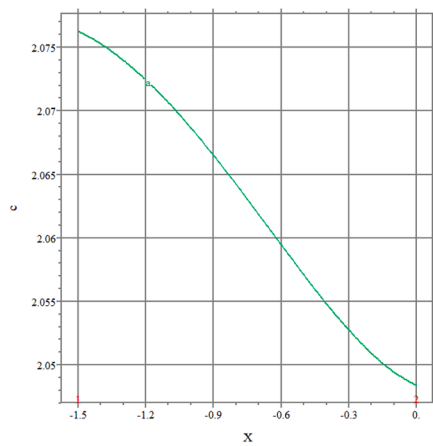
a) Two dimensional graph of concentration changes of component (c) in terms of distance from the center of the vessel to outside the environment for heat source=0.



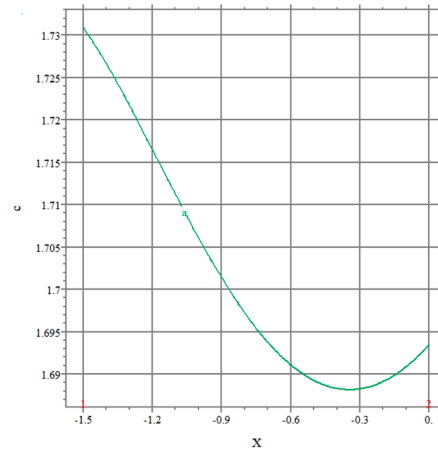
b) Two dimensional graph of concentration changes of component (c) in terms of distance from the center of the vessel to outside the environment for heat source=3.



c) Two dimensional graph of concentration changes of component (c) in terms of distance from the center of the vessel to outside the environment for heat source=5.

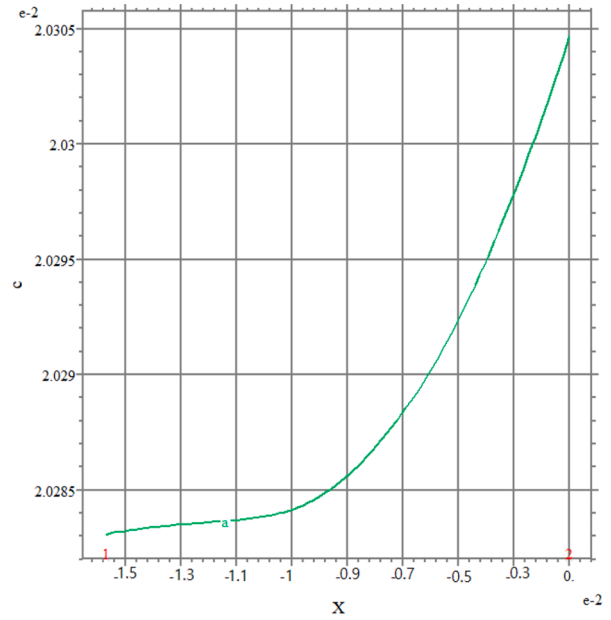
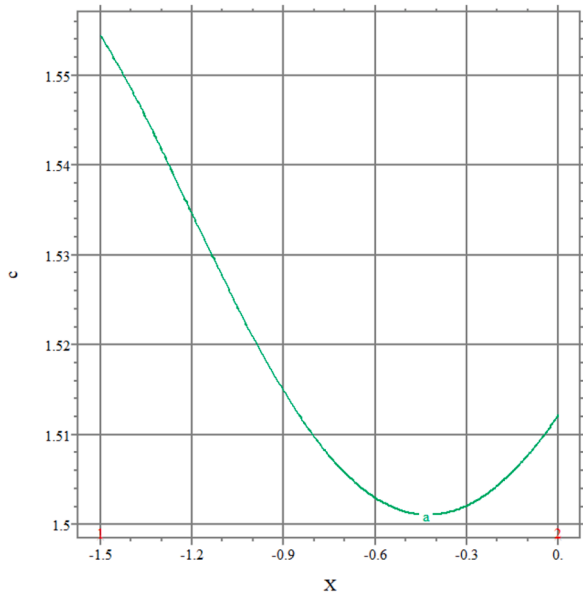


d) Two dimensional graph of concentration changes of component (c) in terms of distance from the top of the vessel to outside the environment for heat source=0.



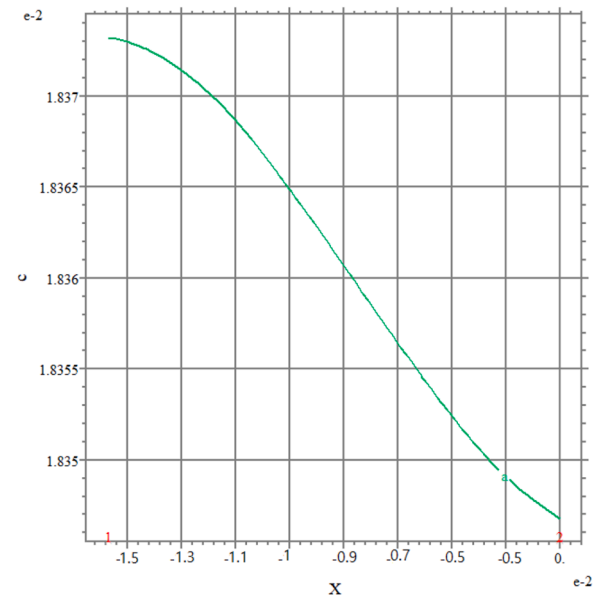
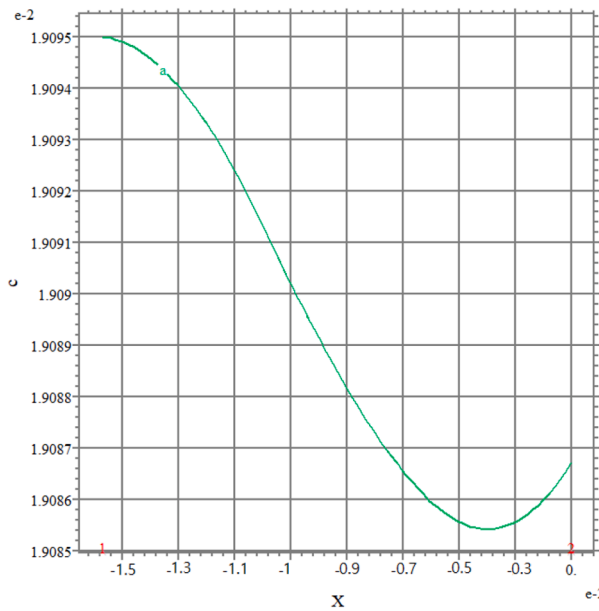
e) Two dimensional graph of concentration changes of component (c) in terms of distance from the top of the vessel to outside the environment for heat source=3.

**Fig 5-c.** Concentration changes of reacting materials for component (c) at certain intervals with different heat sources.



f) Two dimensional graph of concentration changes of component (c) in terms of distance from the top of the vessel to outside the environment for heat source=5.

g) Two dimensional graph of concentration changes of component (c) in terms of distance from the bottom of the vessel to outside the environment for heat source=0.



h) Two dimensional graph of concentration changes of component (c) in terms of distance from the bottom of the vessel to outside the environment for heat source=3.

i) Two dimensional graph of concentration changes of component (c) in terms of distance from the bottom of the vessel to outside the environment for heat source=5.

Fig 5-c. (continued).

inner vessel relative to each other. According to these 3D diagrams, the maximum diffusion mode of substance (c) occurs when the inner vessel is positioned at the lowest point of the larger vessel in the heat source

=5, and the lowest concentration diffusion occurs when the inner vessel is positioned at the highest point of the larger vessel in the heat source=3. The endothermic reaction cannot occur spontaneously but

must be done on the work system for this type of reaction to progress. Of course, when the enthalpy and entropy changes are such that we have negative Gibbs free energy, these reactions also occur spontaneously. When an endothermic reaction absorbs energy, a temperature drop occurs during the response. Endothermic reactions are identified by increased enthalpy (positive enthalpy changes) and a positive sign of energy Fig 5.

The above 2D diagrams show the temperature changes of the substances involved in the chemical reaction around the inner vessel in 3 different states. Diagrams a-5, b-5 and c-5 are related to the temperature changes around the placement of the inner vessel in the center of the outer vessel, considering the states without a heat source and with a heat source, and the general results have been obtained. The maximum temperature of chemically reacting substances occurs in the state of  $x = -0.7$  in the state of  $T = 145$  and the lowest temperature in the state of  $x = -1.5$  and the state of  $T = 40$ . Diagrams d-5, e-5 and f-5 are related to the temperature changes around the placement of the inner vessel in the top of the outer vessel, considering the states without a heat source and with a heat source, and the general results have been obtained. In this mode, the maximum temperature of chemically reacting substances occurs in the state of  $x = -0.7$  in the state of  $T = 211^\circ$  and the lowest temperature in the state of  $x = -1.5$  and the state of  $T = 3^\circ$ . Diagrams g-5, h-5 and i-5 are related to the temperature changes around the placement of the inner vessel in the bottom of the outer vessel, considering the states without a heat source and with a heat source, and the general results have been obtained. In this mode, the maximum temperature of chemically reacting substances occurs in the state of  $x = -0.7$  in the state of  $T = 232^\circ$  and the lowest temperature in the state of  $x = -1.5$  and the state of  $T = 41^\circ$ . By comparing the graphs obtained for the 3 positions of the inner vessel, we conclude that the maximum heat transfer and temperature of the substances involved in the chemical reaction occurs in the position of the inner vessel in the upper part of the larger vessel with heat source = 5. On average, this heat and temperature transfer is 19% higher than the temperature of the reacting material when the inner vessel is placed in the center of the larger vessel and about 32% higher than the temperature of the reacting material when the smaller vessel is placed at the bottom of the larger vessel.

The above 2D diagrams show the concentration changes of the substances involved in the chemical reaction around the inner vessel in 3 different states. Diagrams a-(5-a), b-(5-a) and c-(5-a) are related to the concentration changes around the placement of the inner vessel in the center of the outer vessel, considering the states without a heat source and with a heat source, and the general results have been obtained. The maximum concentration of chemically reacting substances for component (a) occurs in the state of  $x = -0.6$  in the state of  $C = 9.43$  and the lowest concentration in the state of  $x = -1.5$  and the state of  $C = 7.89$ . Diagrams d-(5-a), e-(5-a) and f-(5-a) are related to the concentration changes for component (a) around the placement of the inner vessel in the top of the outer vessel, considering the states without a heat source and with a heat source, and the general results have been obtained. In this mode, the maximum concentration of chemically reacting substances occurs in the state of  $x = -0.6$  in the state of  $C = 11$  and the lowest concentration in the state of  $x = -1.5$  and the state of  $C = 7.54$ . Diagrams g-(5-a), h-(5-a) and i-(5-a) are related to the concentration changes for component (a) around the placement of the inner vessel in the bottom of the outer vessel, considering the states without a heat source and with a heat source, and the general results have been obtained. In this mode, the maximum concentration of chemically reacting substances occurs in the state of  $x = -0.56$  in the state of  $C = 8.8$  and the lowest concentration in the state of  $x = -1.5$  and the state of  $C = 8.12$ . By comparing the graphs obtained for the 3 positions of the inner vessel, we conclude that the maximum concentration changes of the substances involved in the chemical reaction occurs in the position of the inner vessel in the upper part of the larger vessel with heat source = 5. On average, this concentration change is 15% higher than the concentration of the reacting material when the inner vessel is placed in the center of

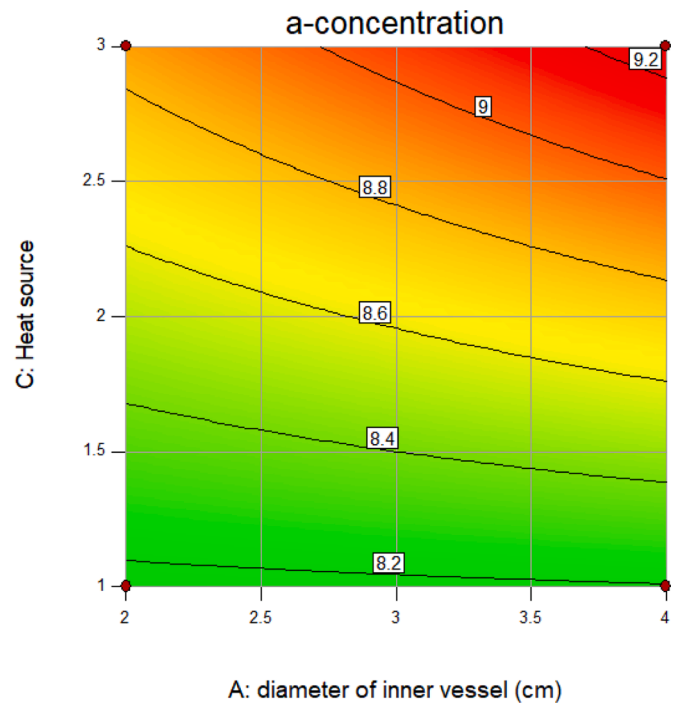


Fig 6. 2D graph RSM method in the a-concentration parameter for range of heat source.

the larger vessel and about 22% higher than the concentration of the reacting material when the smaller vessel is placed at the bottom of the larger vessel.

The above 2D diagrams show the concentration changes of the substances involved in the chemical reaction around the inner vessel in 3 different states. Diagrams a-(5-b), b-(5-b) and c-(5-b) are related to the concentration changes around the placement of the inner vessel in the center of the outer vessel, considering the states without a heat source and with a heat source, and the general results have been obtained. The maximum concentration of chemically reacting substances for component (b) occurs in the state of  $x = -0.6$  in the state of  $C = 9.98$  and the lowest concentration in the state of  $x = -1.5$  and the state of  $C = 9.89$ . Diagrams d-(5-b), e-(5-b) and f-(5-b) are related to the concentration changes for component (b) around the placement of the inner vessel in the top of the outer vessel, considering the states without a heat source and with a heat source, and the general results have been obtained. In this mode, the maximum concentration of chemically reacting substances occurs in the state of  $x = -0.45$  in the state of  $C = 9.99$  and the lowest concentration in the state of  $x = -1.5$  and the state of  $C = 9.92$ . Diagrams g-(5-b), h-(5-b) and i-(5-b) are related to the concentration changes for component (b) around the placement of the inner vessel in the bottom of the outer vessel, considering the states without a heat source and with a heat source, and the general results have been obtained. In this mode, the maximum concentration of chemically reacting substances occurs in the state of  $x = -0.36$  in the state of  $C = 9.95$  and the lowest concentration in the state of  $x = -1.5$  and the state of  $C = 9.52$ . By comparing the graphs obtained for the 3 positions of the inner vessel, we conclude that the maximum concentration changes of the substances involved in the chemical reaction occurs in the position of the inner vessel in the upper part of the larger vessel with heat source = 5. On average, this concentration change is 0.03% higher than the concentration of the reacting material when the inner vessel is placed in the center of the larger vessel and about 0.6% higher than the concentration of the reacting material when the smaller vessel is placed at the bottom of the larger vessel.

The two-dimensional diagrams above depict the concentration changes of the substances involved in the chemical reaction around the

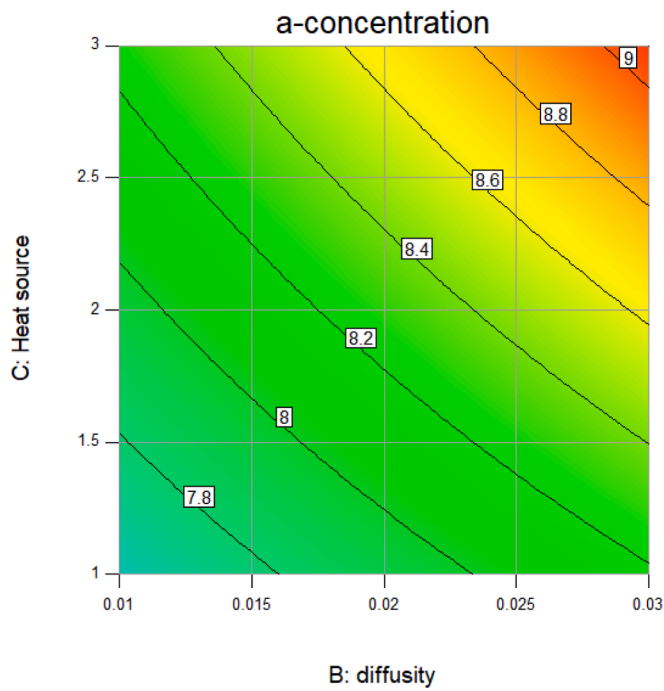


Fig 6-a. 2D graph RSM method in the a-concentration parameter for range of diffusivity.

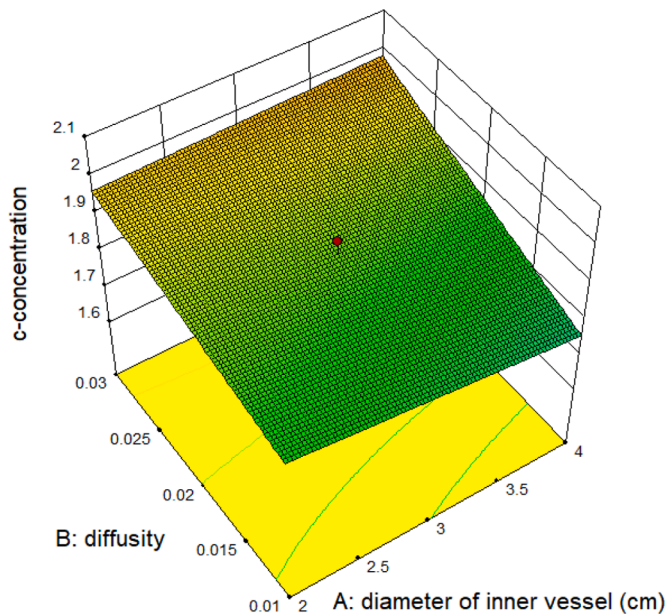


Fig 6-b. 3D graph RSM method in the c-concentration parameter for range of diameter of inner vessel.

inner vessel in three states. The concentration changes around the placement of the inner vessel in the center of the outer vessel, considering the states without and with a heat source, are depicted in diagrams a-(5-c), b-(5-c), and c-(5-c), and general results have been obtained. The highest concentration of chemically reacting substances for component (c) occurs at  $x = -1.4$  and  $C = 2.03$ , while the lowest concentration occurs at  $x = -0.2$  and  $C = 1.63$ . The concentration changes for component (c) around the placement of the inner vessel in the top of the outer vessel, considering the states without and with a heat source, are depicted in diagrams d-(5-c), e-(5-c), and f-(5-c), and general results have been obtained. In this mode, the maximum concentration of

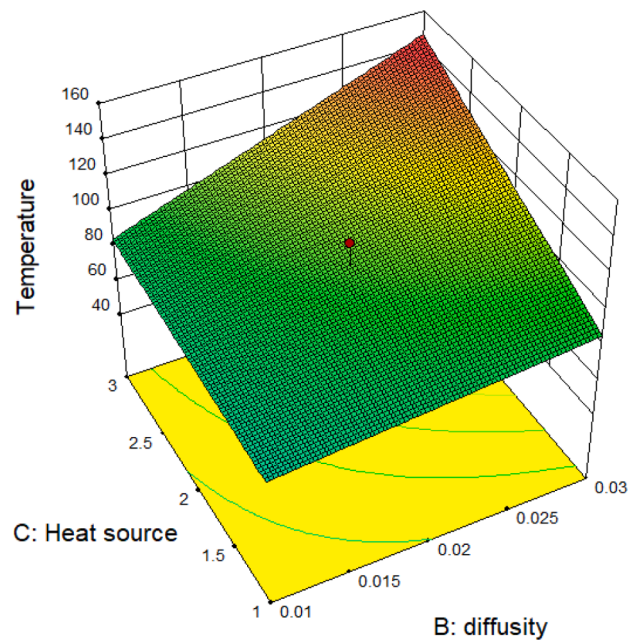


Fig 6-c. 3D graph RSM method in the temperature parameter for range of heat source.

chemically reacting substances occurs in the state of  $x = -1.5$  in the state of  $C = 2.07$  and the lowest concentration in the state of  $x = 0$  and the state of  $C = 1.512$ . Diagrams g-(5-c) · h-(5-c) and i-(5-c) are related to the concentration changes for component (c) around the placement of the inner vessel in the bottom of the outer vessel, considering the states without a heat source and with a heat source, and the general results have been obtained. In this mode, the maximum concentration of chemically reacting substances occurs in the state of  $x = 0$  in the state of  $C = 2.03$  and the lowest concentration in the state of  $x = -1.5$  and the state of  $C = 1.84$ . By comparing the graphs for the three inner vessel positions, we conclude that the maximum concentration changes of the substances involved in the chemical reaction occur in the inner vessel position in the upper part of the larger vessel with heat source = 0. On

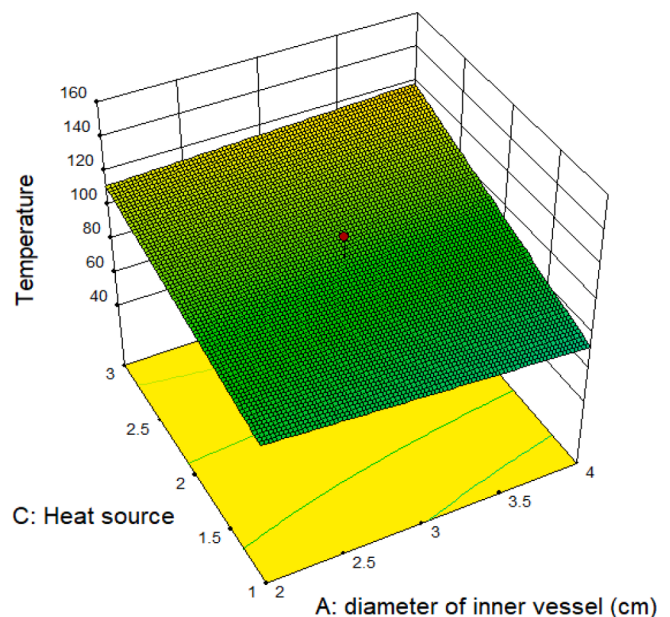


Fig 7. 3D graph RSM method in the temperature parameter for range of diameter of inner vessel.

**Table 2**

The results of 7 tests completed in Design Expert software and the best type of optimization.

Number	diameter	Heat source	diffusivity	a-concentration	b-concentration	c-concentration	temp	Desirability
1	3.144	2.555	0.025	8.687	8.499	1.968	121.06	1.00
2	3.000	2.000	0.020	8.286	8.226	1.887	98.100	1.00
3	4.000	1.000	0.010	7.422	7.620	1.712125	62.975	1.00
4	2.000	3.000	0.010	8.292	8.377	1.795	86.225	1.00
5	4.000	3.000	0.010	8.219	8.161	1.803375	83.975	1.00
6	4.000	3.000	0.030	9.262	8.795	2.117125	154.975	1.00
7	4.000	1.000	0.030	8.194	8.228	1.850875	84.975	1.00

average, this concentration change is 0.18% higher than the concentration of the reacting material when the inner vessel is placed in the center of the larger vessel and about 0.12% higher than the concentration of the reacting material when the smaller vessel is placed at the bottom of the larger vessel.

By using of Design expert software and RSM strategy, we optimize the temperature and concentration of chemical reaction by changing the diameter of the inner vessel and amount of heat sources. Twenty experiments using the RSM technique were carried out in the Design Expert software to obtain the best algorithm results.

The picture above (Fig. 6) shows the changes in material one according to the different changes in the heat source compared to the different diameters of the inner vessel. The range of changes in the heat source is from 1 to 3, and the range of changes in the diameter of the inner vessel is from 2 to 4 cm. By increasing the heat transfer to the center of the inner vessel, the concentration of reactant a in the borders of the vessel increases, so that it reaches from  $c = 8.21$  to  $c = 9.19$ . According to the two-dimensional diagram above, with the increase in the diameter of the vessel, the concentration of the reactant increases, this leads us to the conclusion that with the onset of the thermal boundary layer, the concentration of the reactant also grows, and as the thickness of the boundary layer decreases, the concentration of the substances decreases.

The picture above (Fig. 6-a) shows the changes in material one according to the different changes in the heat source compared to the diffusivity of the inner vessel. The range of changes in the heat source is from 1 to 3, and the range of changes in the diffusivity of the inner vessel is from 0.01 to 0.03. By increasing the heat transfer to the center of the inner vessel, the concentration of reactant a in the borders of the vessel increases, so that it reaches from  $c = 8.21$  to  $c = 9.19$ . According to the two-dimensional diagram above, with the increase in the diffusivity of the reaction components, the concentration of the reactant increases, this leads us to the conclusion that with the increase in the diffusion coefficient, the thermal diffusion of substance increases towards the outside of the boundary layer, and the lower the diffusion coefficient, the lower the heat and concentration.

The picture above (Fig. 6-b) shows the changes in material one according to the different changes in the diffusivity compared to the different diameters of the inner vessel. The range of changes in the diffusivity is from 0.01 to 0.03, and the range of changes in the diameter of the inner vessel is from 2 to 4 cm. The maximum amount of concentration of the produced substance (c) occurs in a state where, in addition to the largest diameter of the inner vessel, we also have the largest thermal diffusion coefficient. The highest value of the concentration of a substance (c) is equal to 1.97 and it occurs in a state where the diffusion coefficient is equal to 0.03 and the size of the diameter of the inner vessel is 4 cm. The minimum concentration value of substance c occurs when the inner vessel has the smallest value have.

The picture above (Fig. 6-c) shows the changes in material one according to the different changes in the diffusivity compared to the different heat source of the inner vessel. The range of changes in the diffusivity is from 0.01 to 0.03, and the range of changes in the heat source of the inner vessel is from 1 to 3. The maximum temperature of chemically reacting substances occurs when we use a heat source, such as the 3D contour above at the heat source point equal to 2.5 and the

chemical diffusion coefficient equal to 0.025, the maximum temperature of the chemical reaction takes place. This position has a temperature of  $140^\circ$ . When we transmit less heat to the center of the plate shape, the least temperature transfer likewise takes place, and the chemical diffusion coefficient also reaches its smallest value.

The picture above (Fig. 7) shows the changes in material one according to the different changes in the heat source compared to the different diameter of the inner vessel. The range of changes in the diameter of the vessel is from 2 cm to 4 cm, and the range of changes in the heat source of the inner vessel is from 1 to 3. Relatively, with the increase in the diameter of the smaller vessel and the increase in the amount of heat transfer, the temperature of the reactive material increases, and the temperature decreases by making the diameter of the inner vessel smaller.

Table 2 shows the results of 7 of the most important tests to optimize the chemical reaction parameters of materials (a), (b), and (c). According to the test conducted with the RSM method, the best efficiency and optimization of temperature and concentration parameters occurs in test number 1.

## 5. Conclusion (Results)

In this manuscript, we explore the temperature and concentration of particles around a vessel in a variety of locations using the reaction and diffusion relations, the reaction among three chemical particles, and the relationship between temperature changes and the rate of chemical reaction. The innovation of this essay is that it compares the parameters of concentration and temperature of substances involved in chemical reactions in different places of the inner vessel to the larger vessel, with and without the presence of a heat source. We also achieved the highest and best efficiency of concentration and heat transfer of chemical reactions (a), (b), and (c) using the finite technique in Flexpde, Ansys fluent, and Design - Expert software (c). The results show that as the temperature of the reactants rises and more heat is released, the concentration and amount change significantly. However, in products such as substance (c), it has an inverse relationship with reactants (a) and (b), such that as the concentration and temperature of the reactants increase, these values in the product decrease.

- In the section of mesh problem, in areas where the lattice density is higher, changes in the concentration and temperature of the materials involved in the chemical reaction are greater.
- The concentration of the reactant also has a direct relationship with the temperature and heat transfer from the system. As the reactant's concentration increases, the reaction's temperature increases, and more energy are released.
- In the case where the inner vessel is placed at the end of the larger vessel (lower part), with the increase of heat transfer to the inner center of the inner vessel, the concentration of the produced substance (c) behind the inner vessel increases from the minimum value to the maximum value, and the viscosity increases.
- According to the test conducted with the RSM method, the best efficiency and optimization of temperature and concentration parameters occurs in heat source=2.555°, diffusivity=0.025 and diameter of inner vessel =3.144 cm.

## Declaration of Competing Interest

The authors declare that they have no known competing financial interests or personal relationships that could have appeared to influence the work reported in this paper.

## Data availability

No data was used for the research described in the article.

## References

- [1] K.M. Owolabi, K.C. Patidar, Higher-order time-stepping methods for time-dependent reaction–diffusion equations arising in biology, *Appl. Math. Comput.* 240 (2014) 30–50, <https://doi.org/10.1016/j.amc.2014.04.055>.
- [2] P. Skrzyżpacz, A. Kadyrbek, B. Golman, V.V. Andreev, Dead-core solutions to fast diffusion-reaction equation for catalyst slabs with power-law reaction kinetics and external mass transfer resistance, *Chem. Eng. J.* (2022), 136722, <https://doi.org/10.1016/j.cej.2022.136722>.
- [3] M. Abdollahzadeh, M. Khosravi, B. Hajipour Khire Masjidi, A. Samimi Behbahan, A. Bagherzadeh, A. Shahkar, F. Tat Shahdost, Estimating the density of deep eutectic solvents applying supervised machine learning techniques, *Sci. Rep.* 12 (1) (2022) 1–16.
- [4] S. Sadeqi, N. Xiros, S. Rouhi, J. Ioup, J. VanZwieten, C. Sultan, Wavelet transformation analysis applied to incompressible flow field about a solid cylinder. ASTFE Digital Library, Begel House Inc, 2021.
- [5] S. Rouhi, N. Xiros, S. Sadeqi, J. Ioup, C. Sultan, J. VanZwieten, CFD validation of the thermodynamics model of a compressed gaseous hydrogen storage tank, *Am. Soc. Therm. Fluids Eng.* (2021). TFEC-2021-36525.
- [6] B. Sobhaniragh, S.H. Afzalimir, C. Ruggieri, Towards the prediction of hydrogen-induced crack growth in high-graded strength steels, *Thin-Walled Structures* 159 (2021), 107245.
- [7] A. Kostka, D. Naujoks, T. Oellers, S. Salomon, C. Somsen, E. Öztürk, G. Eggeler, Linear growth of reaction layer during in-situ TEM annealing of thin film Al/Ni diffusion couples, *J. Alloys Compd.* (2022), 165926, <https://doi.org/10.1016/j.jallcom.2022.165926>.
- [8] R. Fakhimi, M. Shahabsafa, W. Lei, S. He, J.R. Martins, T. Terlaky, L.F. Zuluaga, Discrete multi-load truss sizing optimization: model analysis and computational experiments, *Optimization and Eng.* 23 (3) (2022) 1559–1585.
- [9] M.J. Abdollahzadeh, R. Fathollahi, P. Pasha, M. Mahmoudi, A. Samimi Behbahan, D. Domiri Ganji, Surveying the hybrid of radiation and magnetic parameters on Maxwell liquid with TiO<sub>2</sub> nanotube influence of different blades, *Heat Transf.* 51 (6) (2022) 4858–4881.
- [10] R. Fathollahi, S. Hesaraki, A. Bostani, E. Shahriyari, H. Shafiee, P. Pasha, D. Ganji, Applying numerical and computational methods to investigate the changes in the fluid parameters of the fluid passing over fins of different shapes with the finite element method, *Int. J. Thermofluids* 15 (2022), 100187.
- [11] P. Shadman, Z. Parhizi, R. Fathollahi, M. Zarinfar, E.Y. Anisimova, P. Pasha, Combined septum and chamfer fins on threated stretching surface under the influence of nanofluid and the magnetic parameters for rotary seals in computer hardware, *Alexandria Eng. J.* 62 (2023) 489–507.
- [12] Sima Besharat Ferdosi, Maryam Abasi, Axial buckling of single-walled nanotubes simulated by an atomistic finite element model under different temperatures and boundary conditions, *Int. J. Sci. Eng. App.* 11 (11) (2022) 151–163, <https://doi.org/10.7753/IJSEA1111.1002>. Volume-Issue-ISSN:- 2319 –7560.
- [13] M. Karimzadeh, S.M. Mirtabaei, M. Karimzadeh, S.A. Abdollahi, P. Pasha, D. Ganji, Heat transmission and magnetic effects on a ferrofluid liquid in a hybrid survey under the influence of two Helmholtz coils, *Results in Eng.* (2022), 100702.
- [14] Mahshid Chireh, Mahmoud Naseri, Hamidreza Ghaedamini, Enhanced microwave absorption performance of graphene/doped Li ferrite nanocomposites, *Adv. Powder Technol.* 32 (12) (2021) 4697–4710.
- [15] R. Fatehinasab, H. Shafiee, M. Afshari, P. Pasha, Hybrid surveying of radiation and magnetic impacts on Maxwell fluid with MWCNT nanotube influence of two wire loops, *ZAMM-J. Appl. Math. Mech./Zeitschrift für Angewandte Mathematik und Mechanik* (2022), e202200186.
- [16] P. Pasha, S. Mirzaei, M. Zarinfar, Application of numerical methods in micropolar fluid flow and heat transfer in permeable plates, *Alexandria Eng. J.* (2021), <https://doi.org/10.1016/j.aej.2021.08.040>.
- [17] M. Ikeda, M. Aniya, A measure of cooperativity in non-Arrhenius structural relaxation in terms of the bond strength–coordination number fluctuation model, *Eur. Polym. J.* 86 (2017) 29–40, <https://doi.org/10.1016/j.eurpolymj.2016.11.005>.
- [18] L. Latanowicz, Complex methyl group and hydrogen-bonded proton motions in terms of the Arrhenius and Schrödinger equations, *Solid State Nucl. Magn. Reson.* 34 (1–2) (2008) 93–104, <https://doi.org/10.1016/j.ssnmr.2007.10.001>.
- [19] M. Rufino, S. Guedes, Arrhenius activation energy and transitivity in fission-track annealing equations, *Chem. Geol.* 595 (2022), 120779, <https://doi.org/10.1016/j.chemgeo.2022.120779>.
- [20] O.A. Famakinwa, O.K. Koriko, K.S. Adegbe, A.J. Omowaye, Effects of viscous variation, thermal radiation, and Arrhenius reaction: the case of MHD nanofluid flow containing gyrotactic microorganisms over a convectively heated surface, *Partial Differential Equations in Appl. Mathematics* 5 (2022), 100232, <https://doi.org/10.1016/j.padiff.2021.100232>.
- [21] M. Ebermann, R. Bogenfeld, J. Kreikemeier, R. Glüge, Analytical and numerical approach to determine effective diffusion coefficients for composite pressure vessels, *Compos. Struct.* 291 (2022), 115616, <https://doi.org/10.1016/j.compstruct.2022.115616>.
- [22] K.Milani Shirvan, et al., Numerical investigation and sensitivity analysis of effective parameters on combined heat transfer performance in a porous solar cavity receiver by response surface methodology, *Int. J. Heat Mass Transf.* 105 (2017) 811–825.
- [23] K.M. Shirvan, M. Mamourian, S. Mirzakanlari, R. Ellahi, Numerical investigation of heat exchanger effectiveness in a double pipe heat exchanger filled with nanofluid: a sensitivity analysis by response surface methodology, *Powder Technol.* 313 (2017) 99–111.
- [24] K.M. Shirvan, M. Mamourian, S. Mirzakanlari, R. Ellahi, Two phase simulation and sensitivity analysis of effective parameters on combined heat transfer and pressure drop in a solar heat exchanger filled with nanofluid by RSM, *J. Mol. Liq.* 220 (2016) 888–901.
- [25] A. Majeed, N. Amin, A. Zeeshan, R. Ellahi, S.M. Sait, K. Vafai, Numerical Investigation On Activation Energy of Chemically Reactive Heat Transfer Unsteady Flow With Multiple Slips, *International Journal of Numerical Methods for Heat & Fluid Flow*, 2020.
- [26] A. Abbasi, W. Farooq, E.S.M. Tag-ElDin, S.U. Khan, M.I. Khan, K. Guedri, A. M. Galal, Heat transport exploration for hybrid nanoparticle (Cu, Fe<sub>3</sub>O<sub>4</sub>)—Based blood flow via tapered complex wavy curved channel with slip features, *Micromachines (Basel)* 13 (9) (2022) 1415.
- [27] R. Thejas, C.S. Naveen, M.I. Khan, G.D. Prasanna, S. Reddy, M. Oreijah, M. Jameel, A review on electrical and gas-sensing properties of reduced graphene oxide-metal oxide nanocomposites, *Biomass Conversion and Biorefinery* (2022) 1–11.
- [28] H. Waqas, M. Oreijah, K. Guedri, S.U. Khan, S. Yang, S. Yasmin, A.M. Galal, Gyrotactic motile microorganisms impact on pseudoplastic nanofluid flow over a moving Riga surface with exponential heat flux, *Crystals* 12 (9) (2022) 1308.
- [29] M.F. Ahmed, A. Zaib, F. Ali, O.T. Bafakeeh, E.S.M. Tag-ElDin, K. Guedri, M.I. Khan, Numerical computation for gyrotactic microorganisms in MHD radiative eyring–powell nanomaterial flow by a static/moving wedge with darcy–forchheimer relation, *Micromachines (Basel)* 13 (10) (2022) 1768.
- [30] M. Nazeer, F. Hussain, M.I. Khan, K. Khalid, Theoretical analysis of electrical double layer effects on the multiphase flow of Jeffrey fluid through a divergent channel with lubricated walls, *Waves in Random and Complex Media* (2022) 1–15.
- [31] M. Shahid, H.M.A. Javed, M.I. Ahmad, A.A. Qureshi, M.I. Khan, M.A. Alnuwaier, A. Rafique, A brief assessment on recent developments in efficient electrocatalytic Nitrogen reduction with 2D non-metallic nanomaterials, *Nanomaterials* 12 (19) (2022) 3413.
- [32] N. Manzoor, I. Qasim, M.I. Khan, M.W. Ahmed, K. Guedri, O.T. Bafakeeh, A. M. Galal, Antibacterial Applications of Low-Pressure Plasma on Degradation of Multidrug Resistant V. cholera, *Appl. Sci.* 12 (19) (2022) 9737.
- [33] B. Sehar, A. Waris, S.O. Gilani, U. Ansari, S. Mushtaq, N.B. Khan, E.S.M. Tag-ElDin, The impact of laminations on the mechanical strength of carbon-fiber composites for prosthetic foot fabrication, *Crystals* 12 (10) (2022) 1429.
- [34] M.A. Zahoor Raja, M. Shoaib, R. Tabassum, M.I. Khan, C.G. Jagannatha, C. Gali, Performance analysis of backpropagated networks for entropy optimized mixed convection nanofluid with second-order slip over a stretching surface, *Waves in Random and Complex Media* (2022) 1–23.
- [35] S. Ahmad, O. Dawood, M.M. Lashin, S.U. Khattak, M.F. Javed, F. Aslam, T. M. Alaboud, Effect of coconut fiber on low-density polyethylene plastic-sand paver blocks, *Ain Shams Eng. J.* 101982 (2022).
- [36] O.T. Bafakeeh, K. Raghunath, F. Ali, M. Khalid, E.S.M. Tag-ElDin, M. Oreijah, M. I. Khan, Hall current and solet effects on unsteady MHD rotating flow of second-grade fluid through porous media under the influences of thermal radiation and chemical reactions, *Catalysts* 12 (10) (2022) 1233.
- [37] Y.M. Chu, M.I. Khan, T. Abbas, M.O. Sidi, K.A.M. Alharbi, U.F. Alqsair, M.Y. Malik, Radiative thermal analysis for four types of hybrid nanoparticles subject to non-uniform heat source: keller box numerical approach, *Case Stud. Therm. Eng.* 40 (2022), 102474.